

Electronic ISSN: 1309-0267



**International Journal
of Engineering &
Applied Sciences**

**I
J
E
A
S**

IJEAS

**Volume 9, Issue 1
2017**

Published by Akdeniz University

HONORARY EDITORS

(in Alphabetical)

Atluri, S.N.- University of California, Irvine-USA
David Hui- University of New Orleans, USA
Ferreira, A.- Universidade do Porto, PORTUGAL
Liew, K.M.- City University of Hong Kong-HONG KONG
Lim, C.W.- City University of Hong Kong-HONG KONG
Liu, G.R.- National University of Singapore- SINGAPORE
Malekzadeh, P. – Persian Gulf University, IRAN
Nath, Y.- Indian Institute of Technology, INDIA
Omurtag, M.H. -ITU
Reddy, J.N.-Texas A& M University, USA
Saka, M.P.- University of Bahrain-BAHRAIN
Shen, H.S.- Shanghai Jiao Tong University, CHINA
Sofiyev, A.H.- Suleyman Demirel University- TURKEY
Xiang, Y.- University of Western Sydney-AUSTRALIA
Wang, C.M.- National University of Singapore- SINGAPORE
Wei, G.W.- Michigan State University-USA

EDITOR IN CHIEF:

Ömer Civalek – Akdeniz University civalek@yahoo.com

ASSOCIATE EDITORS:

Hakan ERSOY -Akdeniz University hakanersoy@akdeniz.edu.tr
Ibrahim AYDOĞDU -Akdeniz University aydogdu@akdeniz.edu.tr
Kadir MERCAN -Akdeniz University mercankadir@akdeniz.edu.tr

EDITORIAL BOARD

(The name listed below is not Alphabetical or any title scale)

David Hui- University of New Orleans

Meltem ASİLTÜRK -Akdeniz University meltemasilturk@akdeniz.edu.tr

Süleyman Bilgin -Akdeniz University suleymanbilgin@akdeniz.edu.tr

Ferhat Erdal -Akdeniz University eferhat@akdeniz.edu.tr

Sevil Köfteci -Akdeniz University skofteci@akdeniz.edu.tr

Fuat DEMİR -Süleyman Demirel University fuatdemir@sdu.edu.tr

Metin AYDOĞDU -Trakya University metina@trakya.edu.tr

Ayşe DALOĞLU – KTU aysed@ktu.edu.tr

Candan GÖKCEOĞLU – Hacettepe University cgokce@hacettepe.edu.tr

Oğuzhan HASANÇEBİ – METU oguzhan@metu.edu.tr

Rana MUKHERJİ – The ICAI University

Baki ÖZTÜRK – Hacettepe University

İbrahim ATMACA -Akdeniz University atmaca@akdeniz.edu.tr

Yılmaz AKSU -Akdeniz University

Hakan F. ÖZTOP – Fırat University

Kemal POLAT- Abant İzzet Baysal University

Selim L. SANİN – Hacettepe University

Ayla DOĞAN– Akdeniz University

Engin EMSEN – Akdeniz University

Rifat TÜR – Akdeniz University

Serkan DAĞ – METU

Ekrem TÜFEKÇİ – İTÜ

Fethi KADIOĞLU – İTÜ

Ahmet UÇAR – Gaziantep University

Halit YAZICI – Dokuz Eylül University

Bekir AKGÖZ -Akdeniz University bekirakgoz@akdeniz.edu.tr

Çiğdem DEMİR -Akdeniz University cigdemdemir@akdeniz.edu.tr

Yaghoub Tadi Beni -Shahrekord University

ABSTRACTING & INDEXING



CONTENTS

Comparative Study on Facial Expression Recognition using Gabor and Dual-Tree Complex Wavelet Transforms

By Alaa Eleyan1-13

Development of Pavement Maintenance Management System (PMMS) of Urban Road Network Using HDM-4 Model

By Tanuj Chopra, Manoranjan Parida, Naveen Kwatra, Jyoti Mandhani.....14-31

Utilization of a New Methodology on Performance Measurements of Red Light Violations Detection Systems

By Metin Mutlu Aydin, Sevil Kofteci, Kadir Akgol and Mehmet Sinan Yildirim32-41

Optimisation of Refrigeration System with Two-Stage and Intercooler Using Fuzzy Logic and Genetic Algorithm

By Bayram Kılıç42-54

Frequency and Mode Shapes of Au Nanowires Using the Continuous Beam Models

By Hayri Metin Numanoglu, Kadir Mercan, Ömer Civalak55-61

Comparative Study on Facial Expression Recognition using Gabor and Dual-Tree Complex Wavelet Transforms

Alaa Eleyan

Electrical & Electronics Engineering Department, Avrasya University, Yomra, Trabzon, TURKEY
E-mail address: aeleyan@avrasya.edu.tr

Received date: January 2017

Abstract

Moving from manually interaction with machines to automated systems, stressed on the importance of facial expression recognition for human computer interaction (HCI). In this article, an investigation and comparative study about the use of complex wavelet transforms for Facial Expression Recognition (FER) problem was conducted. Two complex wavelets were used as feature extractors; Gabor wavelets transform (GWT) and dual-tree complex wavelets transform (DT-CWT). Extracted feature vectors were fed to principal component analysis (PCA) or local binary patterns (LBP). Extensive experiments were carried out using three different databases, namely; JAFFE, CK and MUFEE databases. For evaluation of the performance of the system, *k*-nearest neighbor (*k*NN), neural networks (NN) and support vector machines (SVM) classifiers were implemented. The obtained results show that the complex wavelet transform together with sophisticated classifiers can serve as a powerful tool for facial expression recognition problem.

Keywords: facial expression, complex wavelet transform, local binary pattern, principle component analysis, neural networks, support vector machines.

1. Introduction

In recent decades, significant attention of researchers was drawn to the areas of digital image processing, computer vision and pattern recognition. This can be justified as a result of the increase demand of robots in security, entertainment, industry and healthcare related applications [1,2]. In the design of HCI [3], robots and humans can communicate in more natural way if the robots are able to understand human gestures and facial expressions [4]. This can make them respond efficiently and harmonically during tasks where both must work together.

Facial expression is simply a contraction of facial muscles that reflects the emotional state of an individual. Facial Expression Recognition (FER) is an application for automatically identifying a face of a person from an image or a video sequence and compares it with the database to interpret the emotional state of that person. Facial expressions play a significant role in nonverbal human communications. According to the Mehrabian formula; 7%, 38% and 55% of message pertaining to feelings and attitudes is in the spoken words, paralinguistic and in facial expression, respectively [5].

Ekman [6], specified a set of six basic emotions; anger, disgust, fear, happy, sad and surprise which are universal and correlated with muscular patterns in all cultures. Later on, the neutral expression was included as the seventh basic emotion. Generally, the existing approaches to facial expression



recognition is categorized into geometric based approaches [7,8] and appearance based approaches [9,10].

Several algorithms have been introduced and/or improved to reduce the gap between human and computers in accuracy of FER. Currently, Wavelet Transform algorithms such as Discrete Wavelet Transform (DWT), Gabor Wavelet Transform (GWT) and Dual-Tree Complex Wavelet Transform (DT-CWT) are commonly used for feature extraction due to their multi-scale and multi-directional properties. GWT and DT-CWT can demonstrate suitable characteristic of directional selectivity and spatial locality and utilize all the information in space and frequency domain. They also have the advantage of eliminating the effect of non-uniform illumination in a face image.

The DWT is a well-known algorithm for feature extraction. However, it lacks good directional selectivity, shift variance sensitivity and phase information. GWT, on the other hand, can overcome those limitations. It has been extensively used in the field of image processing and computer vision applications. The Gabor wavelet filter is an essential tool used to capture and extract local features both in spatial and frequency domain aligned at particular directions and scales [11, 12].

Lyons *et al.* [13] proposed an approach for automatic facial images classification based on labelled elastic graph matching and GWT. The work conducted in [14, 11], claimed that biological relevance of GWT makes it a powerful tool as a feature extractor. Researchers in [15] used GWT as a feature extraction technique for palmprint recognition while in [16] they enhanced the fingerprint images using GWT.

However, GWT suffers from its high computational complexity and huge memory requirement to store the large feature vectors extracted. For instance, for an image of size 256×256 , with a Gabor filter of 5 scales and 8 directions, the 40 magnitude responses reside in $256 \times 256 \times 40$ (2621440) dimensional space which is very huge and requires a large storage capacity.

The popularly known DT-CWT introduced by Kingsbury [17], imitates Gabor wavelet kernels and provides good directional selectivity in 6 fixed directions at different scales. Furthermore, the DT-CWT has some added advantages such as its limited redundancy for image and it is much computationally faster than Gabor wavelets; hence it serves as a perfect replacement for Gabor wavelet filter. Thus, with DT-CWT we can get a comparable performance with less computational complexity. Researchers in [18, 19] applied DT-CWT to enhance the face recognition performance. Sun *et al.* [20] used DT-CWT for face detection using spectral histogram. Y. Wang in [21], investigated the application of the DT-CWT based on local binary pattern weighted histogram method for palmprint recognition. In [22], DT-CWT and SVM was used for the image de-noising problem. Moreover, DT-CWT was also used in [23] with SVM for handwritten numeral recognition. Face recognition problem was addressed in [24] using three different complex wavelet transforms. Researchers in [25] used DT-CWT for facial expression recognition together with supervised spectral analysis.

The rest of the article is organized as follows. Sections 2 and 3 gives a brief overview of GWT & DT-CWT. The two dimensionality reduction algorithms are described in section 4. Section 5 discusses the proposed approach, while Section 6 gives the simulation results and discussions. Finally, section 7 contains drawn conclusions.

2. Complex Wavelets Transforms

2.1. Gabor Wavelet Transform

It is well established that the scales and directions of the GWT are similar to that of the primary visual cortex of the mammalian brain [26]. GWT is widely used in many pattern recognition analyses. The GWT extracts the features of the input image that are aligned at particular directions and scales.

GWT possesses many properties which makes it suitable for different applications. It has good directional selectivity and is insensitive to illumination variations. A 2D Gabor filter can be defined in both spatial and frequency domain as [27]:

$$\Psi_{u,v}(x, y) = \frac{f_u^2}{\pi\kappa\eta} e^{-\left(\frac{f_u^2}{\kappa^2}x'^2 + \frac{f_u^2}{\eta^2}y'^2\right)} e^{j2\pi f_u x'} \quad (1)$$

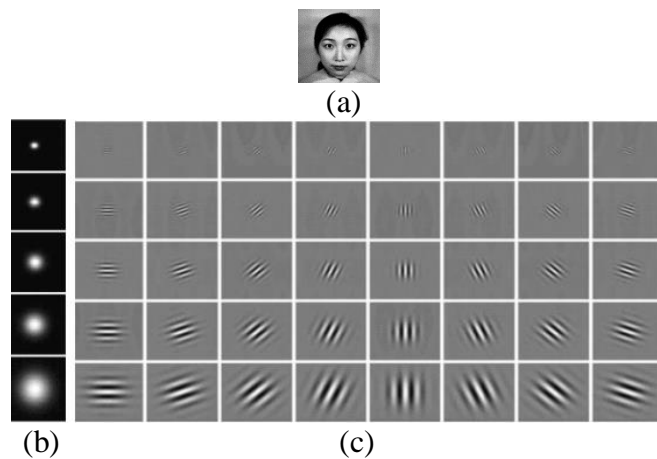
where (x, y) are the coordinates of the pixel's values, $x' = x\cos\theta_v + y\sin\theta_v$, $y' = -x\sin\theta_v + y\cos\theta_v$ and (x', y') are the new coordinates of the pixel values after anti clockwise rotation from the old coordinates (x, y) .

$$\begin{aligned} f_u &= f_{max}/\sqrt[5]{2} \\ \theta_v &= v\pi/8 \end{aligned}$$

f_u is the center frequency of the complex sinusoid, $\sqrt[5]{2}$ is the spacing factor between different central frequencies and θ_v is the orientation of the wavelet. The κ and η are the sharpness along the minor and the major axis of the Gaussian envelop. The commonly used values for face and facial expression recognition are $\kappa = \eta = \sqrt{2}$ and $f_{max} = 0.25$ with a scale of 5 ($u = 0,1,2,3,4$) and orientation of 8 ($v = 0,1,2,3,4,5,6,7$) [28,29]. If $\mathbf{I}(x, y)$ is the face image of size $N \times M$ and $\Psi_{u,v}(x, y)$ is the Gabor filter, then the feature extraction which is the filtering operation of the image and the Gabor filter can be defined as:

$$\mathbf{G}_{u,v}(x, y) = \mathbf{I}(x, y) * \Psi_{u,v}(x, y) \quad (2)$$

where $\mathbf{G}_{u,v}(x, y)$ represents the output of the filtering process and $*$ is the convolution operator. Fig. 1 shows example of an image to be filtered, magnitude and real parts of the Gabor wavelets filters at 5 scales and 8 directions and the magnitude of the output obtained after filtering.



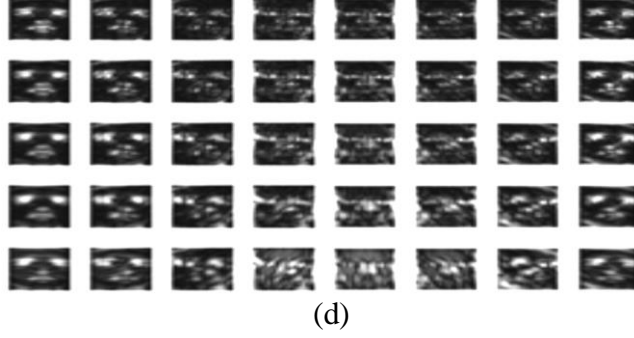


Fig. 1. (a) Image to be filtered (b) Magnitude of Gabor filter at 5 scales and (c) Real parts at 5 scales and 8 directions of the Gabor wavelets filters and (d) Magnitude of the output obtain after convolution.

2.2. Dual-Tree Complex Wavelet Transform

The DT-CWT possesses similar shapes to Gabor Wavelets Transform [17]. As shown in Fig. 2, the DT-CWT contains two trees of real filters, tree ‘a’ and tree ‘b’, which give the real and imaginary parts of the complex coefficients.

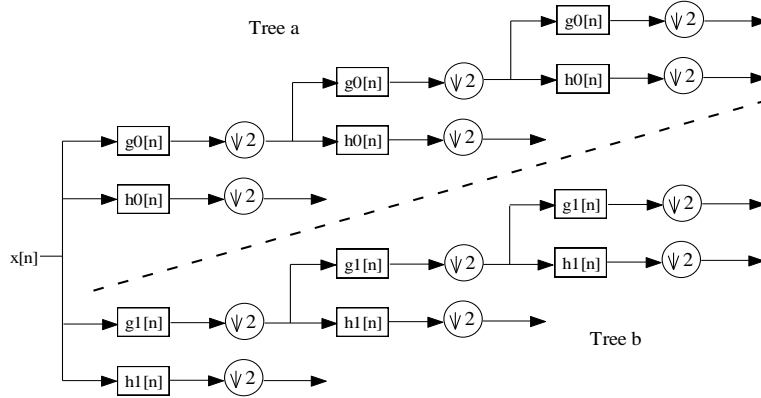


Fig. 2. Dual-Tree Complex Wavelet Transform [17].

Kingsbury summarized the properties of DT-CWT as: approximate shift invariance, good directional selectivity in 2-D with Gabor-like filters, perfect reconstruction using short linear-phase filters, limited redundancy, independent of the number of scales, and efficient order-N computation.

The DT-CWT filters used are designed to give perfect reconstruction at every scale. The transform has the ability to differentiate positive and negative frequencies and produce six sub-bands strongly oriented in $\pm 15^\circ$, $\pm 45^\circ$, and $\pm 75^\circ$ as shown in Fig. 3(c). However, unlike Gabor wavelet transform where the sub-band can be computed in any orientation, here the directions are fixed. The DT-CWT expansion of an image $\mathbf{f}(\vec{x})$ is given by:

$$\mathbf{f}(\vec{x}) = \sum_k \mathbf{W}_\varphi(j_o, k) \boldsymbol{\varphi}_{j_o, k}(\vec{x}) + \sum_i \sum_{j > j_o} \sum_k \mathbf{W}_\psi(j, k) \boldsymbol{\Psi}_{j, k}^i(\vec{x}), \quad (3)$$

where $i = \pm 15^\circ, \pm 45^\circ, \text{ and } \pm 75^\circ$. The scaling function $\phi_{j_o,k}$ and the wavelet function $\psi_{j,k}^i$ are complex. $\mathbf{W}_\phi(j_o,k)$ indicates the scaling coefficients and $\mathbf{W}_\psi(j,k)$ are wavelet coefficients of the transform. Fig. 3 shows face image from JAFFE database, the real part and magnitude of impulse response of DT-CWT and the magnitude response obtained for JAFFE face image using DT-CWT at 3 scales and 6 fixed directions ($\pm 15^\circ, \pm 45^\circ$ and $\pm 75^\circ$).

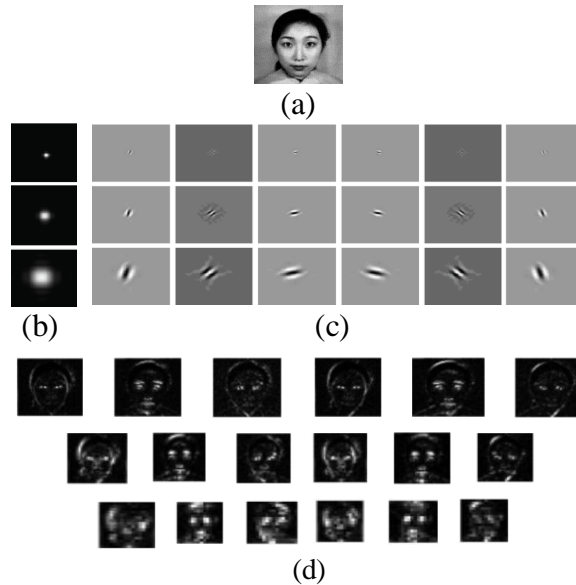


Fig. 3. (a) Face image from JAFFE database (b) Magnitude of the DT-CWT filter response (c) Real part of DT-CWT filter response at 3 scales and 6 directions. (d) The magnitude response obtained for JAFFE face image using DT-CWT for 3 scales and 6 directions

The dimensions of the feature vectors created by GWT and DT-CWT are huge as such dimensionality reduction is usually employed by linearly combining the feature vectors and projecting the high dimensional features onto a lower dimensional space [28,29].

3. Dimensionality Reduction

3.1. Principal Component Analysis

Principle Component Analysis (PCA) is one of the classical techniques used to find the effective linear transformations. PCA is extensively used in signal processing and pattern recognition applications for feature extractions and data dimensionality reduction [10]. In this article, PCA was used to reduce the dimensionality of the GWT and DT-CWT feature vectors. For further details regarding PCA algorithm reader should return to [10].

3.2. Local Binary Patterns

Even though LBP is a feature extraction algorithm rather than being a tool for dimensionality reduction, we benefited from its working mechanism to reduce the dimensionality of the feature vectors generated using wavelet transforms. The LBP algorithm [30] is dividing the face image into

non-overlapping regions. For each region, a 3×3 neighborhood is defined. The neighboring pixels are examined based on the central pixel grayscale value which threshold the neighbors to 1 or 0. Hence an 8-bit binary string representing each pixel will be formed which will be converted to a decimal number. Histograms of 256 bins or less for every region will be formed based on the obtained decimal numbers. These histograms are then concatenated to form the feature vector for the face image. An example of the basic LBP operator is shown in Fig. 4.

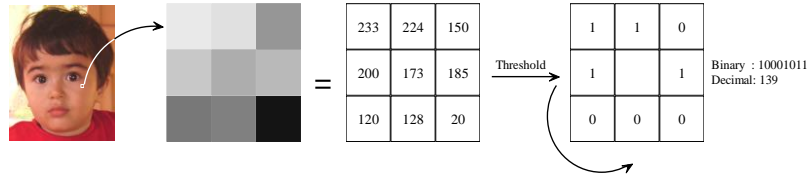


Fig. 4. Example of 3×3 Basic LBP operators.

4. The Proposed Approach

The proposed approach for facial expression recognition is shown in Fig. 5.

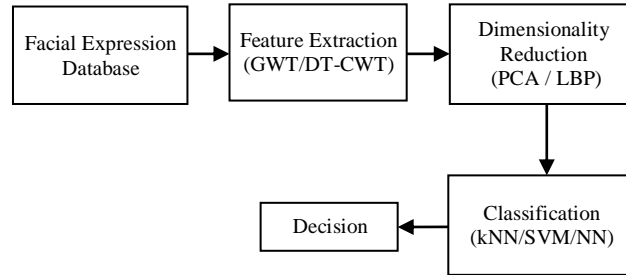


Fig. 5. Block diagram of the proposed approach.

Facial expression database contains the images that will be used both for training and testing. Feature extraction computes salient features (feature vectors) from the face so that redundant information can be discarded. The features of the GWT were extracted using 5 scales and 8 directions. While the DT-CWT salient features were extracted using 3 scales and 6 directions. LBP and PCA were used to reduce the dimensionality of feature vectors of GWT and DT-CWT. A uniform LBP was used where each image is divided into 16 regions with radius $R=1$. kNN, SVM and NN classifiers were used for the classification stage.

4.1. The Databases Used

For evaluating of the proposed approach extensive experiments were carried out on 3 different databases. The first database, The JAFFE database [31] contains 213 images of 10 different females each with 7 basic facial expressions namely; anger (AN), disgust (DI), fear (FE), happy (HA), sad (SA), surprise (SU) and neutral (NE). Resolution of the images is 256×256 pixels. Examples of images from JAFFE database are shown in Fig. 6.



Fig. 6. Examples of images from the JAFFE database.

The second database, Cohn-Kanade (CK) database [32] contains 486 image sequences posed across 97 subjects. Each of the sequence contains images from onset (neutral frame) to peak expression (last frame) and a resolution of 640×490 pixels. The images consist of 12-16 frames. The ages of the subjects ranged from 18-30 years of which 65% were female and 35% were male. Images were resized to 256×256 pixels. Fig. 7 shows examples of image sequences in Cohn-Kanade database.



Fig. 7. Examples of Images from CK Database.

Third database is Mevlana University Facial Expression (MUFE) database [33]. The facial expressions of 15 students were taken at Mevlana University. The database contains 630 facial images of 15 individuals with 80% males and 20% females. Each of the basic 7 facial expressions was recorded 6 times for each subject (2 frontal images, 2 images with subject looking slightly to the right of the camera and 2 images with subject looking slightly to the left of the camera). All the images in the database were manually cropped and resized to 256×256 pixels. Fig. 8 shows examples of images from MUFE database.



Fig. 8. Examples of images from MUFE database.

5. Simulation Results & Discussions

The proposed approach was implemented on JAFFE, MUFE and CK facial expression databases using person-dependent approach and 10-fold cross validation under MATLAB environment. For JAFFE database, 137 of the images were used as training set while 76 images used as testing set. On the other hand, for MUFE database, 50% of the images were used for both training and testing set. 97

subjects from CK database were used making a total of 2716 images with four images per expression per subject. Here three images per subject per expression were used for training, thus, 2037 training images, while one image per subject per expression was used for testing, which gives a total of 679 testing images. GWT and DT-CWT were implemented in three different scenarios. First scenario was implemented using the generated feature vectors directly, while in second and third scenarios feature vectors lengths were reduced using PCA or LBP algorithms before classification. Neural networks with multilayer feed-forward architecture and back propagation learning algorithm and SVM with radial basis function (RFB) kernel were used in our implementation. The results of all the experiments are given in the following tables. Table 1 shows the recognition performance using the 3 facial expression databases. Comparisons between kNN and SVM classifiers are shown for GWT, GWT+PCA and GWT+LBP approaches. Comparisons were conducted on each facial expression separately. The average recognition performance for each database was also recorded in the last row of the table. GWT+PCA+SVM approach recorded the best average performance among other approaches. This result was consistent for the three databases used.

Table 1. Facial expression recognition for GWT using three facial expression databases.

Facial Expression	GWT / GWT+PCA / GWT+LBP					
	JAFPE		MUFEE		CK	
	kNN	SVM	kNN	SVM	kNN	SVM
AN	91.03 / 82.10 / 90.95	89.88 / 99.56 / 90.11	80.93 / 92.21 / 68.76	93.20 / 92.42 / 69.04	76.98 / 92.20 / 96.84	96.86 / 96.97 / 92.07
DI	82.89 / 67.21 / 92.11	91.23 / 91.04 / 91.00	90.79 / 88.65 / 80.23	89.12 / 92.28 / 85.15	96.86 / 96.97 / 96.42	87.01 / 96.97 / 96.53
FE	75.13 / 58.24 / 75.09	91.88 / 91.87 / 92.30	80.32 / 80.02 / 66.79	77.78 / 79.00 / 79.92	87.30 / 91.64 / 76.98	82.64 / 91.53 / 87.12
HA	90.05 / 69.91 / 100.0	83.13 / 92.17 / 91.84	78.76 / 90.28 / 78.18	91.34 / 92.33 / 78.31	86.88 / 87.17 / 87.00	92.31 / 96.97 / 96.97
SA	91.19 / 63.30 / 81.93	81.92 / 100.0 / 99.95	83.23 / 91.40 / 83.88	90.65 / 91.17 / 82.89	96.53 / 96.97 / 88.30	89.77 / 87.20 / 89.40
SU	90.08 / 89.90 / 90.22	100.0 / 100.0 / 90.89	88.69 / 86.15 / 71.20	89.56 / 97.64 / 75.19	87.00 / 96.97 / 86.64	96.53 / 96.97 / 96.97
NE	100.0 / 99.94 / 100.0	100.0 / 99.76 / 100.0	82.37 / 93.37 / 76.09	92.76 / 96.78 / 82.11	96.97 / 96.84 / 96.97	96.97 / 96.97 / 96.75
Avg	88.62 / 75.80 / 90.04	91.15 / 96.33 / 93.73	83.58 / 88.87 / 75.02	89.20 / 91.66 / 78.95	89.79 / 94.12 / 89.88	91.73 / 94.80 / 93.69

Same experiment setup was carried out in Table 2 with the replacement of GWT with DT-CWT. Comparisons between kNN and NN classifiers are shown for DT-CWT, DT-CWT+PCA and DT-CWT+LBP approaches. The average recognition performance for each database was also recorded in the last row of the table. GWT+PCA+NN approach recorded the best average performance among other approaches. In general, kNN classifier, as expected, recorded lower performances than SVM and NN classifiers for the three databases in all scenarios.

Table 2. Facial expression recognition for DT-CWT using three facial expression databases.

Facial Expression	DT-CWT / DT-CWT+PCA / DT-CWT+LBP					
	JAFPE		MUFEE		CK	
	kNN	NN	kNN	NN	kNN	NN
AN	99.78 / 100.0 / 80.45	57.56 / 91.44 / 100.0	80.16 / 67.76 / 64.35	75.40 / 84.54 / 80.95	85.60 / 94.46 / 97.05	87.50 / 87.64 / 92.05
DI	91.23 / 73.34 / 90.56	99.67 / 90.56 / 92.37	82.26 / 82.23 / 80.12	59.41 / 89.95 / 89.32	96.59 / 91.05 / 94.68	96.51 / 97.05 / 96.44
FE	83.12 / 74.78 / 67.67	76.34 / 92.13 / 80.17	76.23 / 52.78 / 70.67	76.66 / 79.51 / 82.83	94.34 / 94.49 / 94.17	87.76 / 87.61 / 82.93
HA	74.78 / 57.89 / 66.56	52.88 / 99.56 / 94.78	79.36 / 62.13 / 71.16	50.25 / 99.94 / 77.05	99.75 / 95.06 / 99.95	97.35 / 97.04 / 96.95
SA	64.33 / 73.34 / 45.02	65.17 / 100.0 / 99.67	80.21 / 76.18 / 80.25	59.84 / 78.37 / 88.47	95.16 / 91.63 / 92.53	96.94 / 96.47 / 96.57
SU	99.67 / 100.0 / 80.45	77.45 / 99.89 / 90.56	84.03 / 76.23 / 79.68	71.85 / 87.05 / 77.29	96.15 / 99.95 / 99.71	86.89 / 96.69 / 97.29
NE	99.78 / 90.15 / 100.0	59.78 / 91.39 / 85.15	86.56 / 63.56 / 76.33	48.96 / 73.90 / 73.75	95.04 / 84.10 / 91.25	96.78 / 97.00 / 96.84
Avg	87.53 / 81.36 / 75.82	69.84 / 95.00 / 91.81	81.26 / 68.70 / 74.65	63.19 / 84.75 / 81.38	91.62 / 89.92 / 92.58	92.82 / 94.21 / 94.15

In Fig. 9, comparisons with the well-known feature extraction algorithms scale-invariant feature transform (SIFT) [34] and speeded up robust features (SURF) [35] are performed on the three databases. In general, the average numbers of key points obtained for an image are 36 and 16 key points using SIFT and SURF, respectively. SIFT performance was slightly better than SURF for the three databases. Still, GWT as a feature extractor recorded the best performance among other algorithms for all databases.

Comparisons with other works conducted on the JAFFE database is shown in Table 3. To the best of our knowledge, all the algorithms available in this table, except algorithm in [39], used person-dependent approach in their simulations. The number inside the parentheses next to recognition rates indicates the number of facial expressions used. If the number is equal to 6 it means the neutral facial expression was neglected.

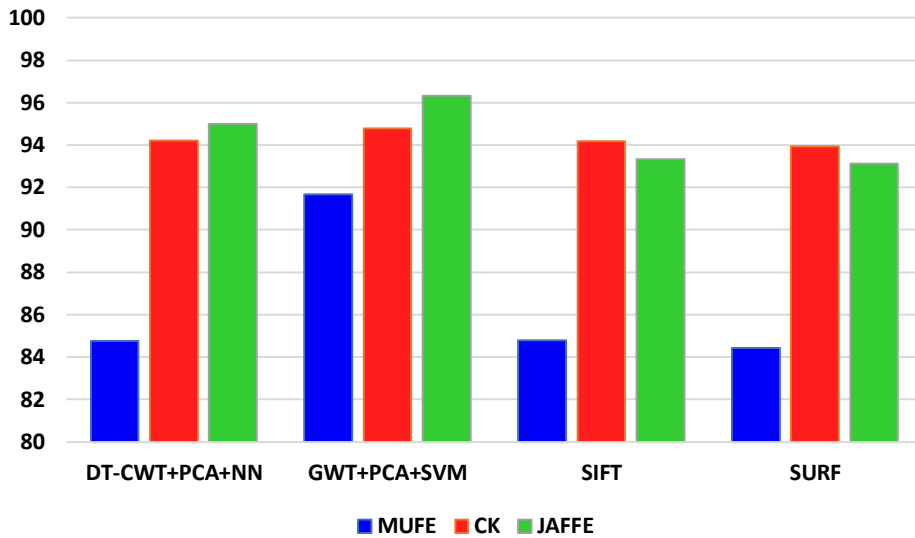


Fig. 9. Facial expression recognition comparison for MUFE, CK and JAFFE databases using different algorithms.

Fig. 10 shows the general average recognition performances of the 7 facial expressions from table 1 and table 2. Averages were calculated using all the algorithms and databases results. It is clearly obvious that disgust (DI), surprise (SU) and neutral (NE) expressions got the highest average recognition performances (>89%). Fear (FE) expression recorded the worst average recognition performance (~81%). Justification of low recognition performance of fear expression might be that sometimes fear expression can be close to surprise expression.

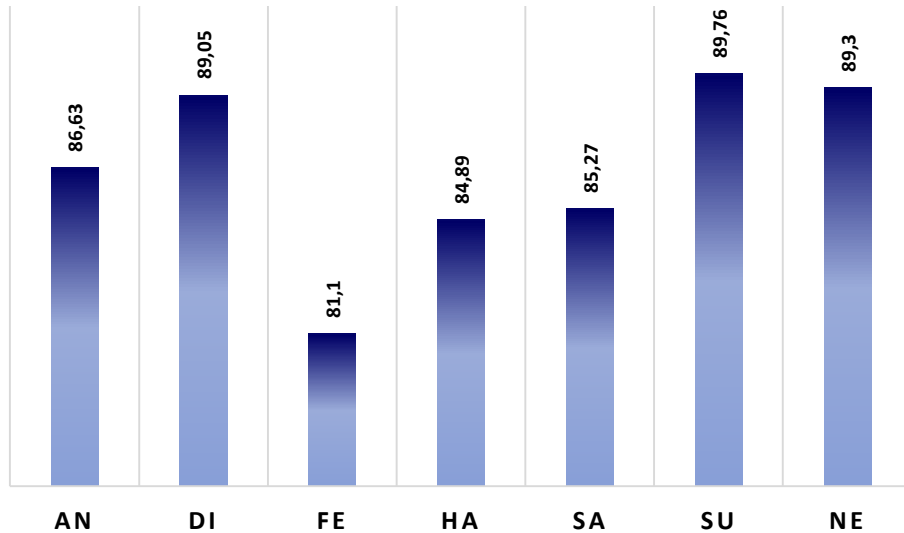


Fig. 10. Average recognition performances of the 7 facial expressions from all applied algorithms and databases.

Table 3. Facial expression recognition performance comparisons for JAFFE database (the listed results are the best recorded results in the respective articles)

Algorithm	Recognition rates
Lyons et al. [34]	92.00% (7)
Zhang et al. [35]	90.10% (7)
Buciu et al. [36]	90.34% (7)
Dubuisson et al. [37]	87.60% (6)
Shinohara & Otsu [38]	69.40% (7)
Kung et al. [39]	68.85% (6)
Happy & Routray [40]	87.43% (6)
Shih et al. [41]	95.71% (7)
DT-CWT+PCA+NN	95.00% (7)
GWT+PCA+SVM	96.33 % (7)

6. Conclusions

This work investigated facial expression recognition problem using GWT and DT-CWT with kNN, SVM and NN classifiers using person-dependent approach. PCA and LBP algorithms were used to reduce the dimensions of the feature vectors generated using GWT and DT-CWT. GWT+PCA with SVM classifier recorded the best average recognition rates of 96.33%, 91.66% and 94.8% for JAFFE, MUFEE and CK databases, respectively. Experimental results obtained demonstrated the high performance and advantage of using DT-CWT in FER problem. The recorded best average recognition rates DT-CWT with NN are 95%, 84.75% and 94.21% for JAFFE, MUFEE and CK

databases, respectively. The overall performance of NN and SVM were, as expected, better than the kNN in all scenarios. Also, the importance of applying dimensionality reduction on the feature vectors before classification stage was realized, where in most experiments the performance increased after applying dimensionality reduction. Finally, it could be seen that the accuracy of the proposed MUFE database is lower than the other databases; firstly, this is due to the fact that MUFE database consist of not only frontal face images but also from slightly left and right orientations of the faces. This is unlike JAFFE and CK where only frontal face images are recorded. Secondly, the participants were not professional actors, hence didn't always give as perfect expressions as desired.

References

- [1] Niu Z., Qiu X., Facial expression recognition based on weighted principal component analysis and support vector machines, *IEEE 3rd International Conference on Advanced Computer Theory and Engineering*, 174-178, 2010.
- [2] Song K.T., Chen Y.W., A design for integrated face and facial expression recognition, *37th Annual conference on IEEE Industrial Electronics Society*, 4306-4311, 2011.
- [3] Vinciarelli A., Pantic M., Bourlard H., Social signal processing survey of an emerging domain, *Image and Vision Computing*, 1743-1759, 2009.
- [4] Lin D., Facial expression classification using PCA and hierarchical radial basis function network, *Journal of Information Science and Engineering*, 22(5), 1033-1046, 2006.
- [5] Mehrabian A., Communication without words, *Psychology Today*, 2(4), 53-56, 1968.
- [6] Ekman P., Friesen W., Facial action coding system: a technique for the measurement of facial movements, *Consulting Psychologists Press*, California, 1978.
- [7] Yacoob Y., Davis L.S., Recognizing human facial expression from long image sequences using optical flow, *IEEE Transactions on Pattern Analysis and Machine Intelligence*, 18(6), 636-642, 1996.
- [8] Brunelli R., Poggio T., Face recognition: features vs. templates, *IEEE Transaction on Pattern Analysis and Machine Intelligence*, 15(10), 1042-1053, 1993.
- [9] Eleyan A., Demirel H., Performance comparison among complex wavelet transforms based face recognition systems, *Image Processing and Communication Conference*, AISC84, 201-209, 2010.
- [10] Turk M., Pentland A., Eigenfaces for recognition, *Journal of Cognitive Neuroscience*, 3(1), 71-86, 1991.
- [11] Abdulrahman M., Gwadabe T. R., Abdu F. J., Eleyan A., Gabor wavelet transform based facial expression recognition using PCA and LBP. In *IEEE 22nd Signal Processing and Communications Applications Conference (SIU)*, 2265-2268, 2014.
- [12] Lee T. S., Image representation using 2d Gabor wavelets, *IEEE Transactions on Pattern Analysis and Machine Intelligence*, 18(10), 959-971, 1996.
- [13] Lyons M. J., Budynek J., Akamatsu S., Automatic classification of single facial images, *IEEE Transactions on Pattern Analysis and Machine Intelligence*, 21(12), 1357-1362, 1999.
- [14] Gu W., Xiang C., Venkatesh Y., Huang D., Lin H., Facial expression recognition using radial encoding of local Gabor features and classifier synthesis, *Pattern Recognition*, 45(1), 80-91, 2012.
- [15] Kong W. K., Zhang D., W. Li, Palm print feature extraction using 2-d Gabor filters, *Pattern Recognition Society*, 2339-2347, 2003.
- [16] Karimimehr N., Sharazi A. A. B., Kashavar B. M., Finger print image enhancement using Gabor wavelet transform, *18th Iranian Conference on Electrical Engineering Proceeding*, 316-320, 2010.

- [17] Kingsbury N. G., The dual-tree complex wavelet transform: a new efficient tool for image restoration and enhancement, *European Signal Processing Conference*, 319-322, 1998.
- [18] Eleyan A., Demirel H., Ozkaramanli H., Face recognition using dual-tree wavelet transform, *IEEE International Symposium on Signal Processing and Information Technology*, 7–11, 2008.
- [19] Liu C.C., Dai D.Q., Face recognition using dual-tree complex wavelet features, *IEEE Transactions on Image Processing*, 18(11), 2593-2599, 2009.
- [20] Sun Y.H., Du M.H., Face detection using dt-cwt on spectral histogram. *IEEE Proceedings, Fifth International Conference on Machine Learning and Cybernetics*, 3637-3642, 2006.
- [21] Wang Y., Dual-tree complex wavelet transform based local binary pattern weighted histogram method for palm print recognition, *Computing and Informatics*, 28, 299-318, 2009.
- [22] Zhang S., Tang T., Wu C., Xi N., Wang G., A novel image denoising method using independent component analysis and dual-tree complex wavelet transform, *6th International Conference on Wireless Communications Networking and Mobile Computing*, 1-4, 2010.
- [23] Chen G. Y., Xie W. F., Pattern recognition using dual-tree complex wavelet features and svm, *Canadian Conference on Electrical and Computer Engineering*, 2053-2056, 2005.
- [24] Eleyan A., Özkaramanli H., Demirel H., Complex wavelet transform-based face recognition, *EURASIP Journal on Advances in Signal Processing*, 2008(1), 1-13, 2009.
- [25] Li Y., Ruan Q., An G., Li X., Facial expression recognition based on the dual-tree complex wavelet transform and supervised spectral analysis, *IEEE 10th International Conference on Signal Processing (ICSP)*, 1301-1304, 2010.
- [26] Daugman J., Uncertainty relation for resolution in space, spatial frequency and orientation optimized by two-dimensional visual cortical filters. *Journal of the Optical Society of America A*, 2(7), 1160-1169, 1985.
- [27] Struc V., Pavesic N., Gabor-based kernel partial least squares discrimination features for face recognition, *Informatica*, 20(1), 115–138, 2009.
- [28] Liu C., Wechsler H., Gabor feature based classification using the enhanced fisher linear discriminant model for face recognition, *IEEE Transactions on Image Processing*, 11(4), 467–476, 2002.
- [29] Shen L., Bai L., Fairhurst M., Gabor wavelets and general discriminant analysis for face identification and verification, *Image and Vision Computing*, 25(5), 553–563, 2007.
- [30] Ojala T., Pietikainen M., Maenpaa T., Multi-resolution gray scale and rotation invariant texture analysis with local binary patterns, *IEEE Transactions on Pattern Analysis and Machine Intelligence*, 24(7), 971-987, 2010.
- [31] Lyons M. J., Akemastu S., Kamachi M., Gyoba J., Coding facial expressions with Gabor wavelets, *3rd IEEE International Conference on Automatic Face and Gesture Recognition*, 200-205, 1998.
- [32] Lucey P., Cohn J.F., Kanade T., Saragih J., Ambadar Z., Matthews I., The extended Cohn-Kande dataset (CK+): A complete facial expression dataset for action unit and emotion-specified expression, *3rd IEEE Workshop on CVPR for Human Communicative Behaviour Analysis*, 94-101, 2010.
- [33] Abdulrahman M., Eleyan A., Facial expression recognition using support vector machines, *23rd IEEE International Signal Processing and Communication Applications Conference (SIU)*, 276-279, 2015.
- [34] Lyons M., Budynek J., Akamatsu S., Automatic classification of single facial images, *IEEE Transaction on Pattern Analysis and Machine Intelligence*, 21(12), 1357–1362. 1999
- [35] Zhang Z., Lyons M., Schuster M., Akamatsu S., Comparison between geometry based and Gabor-wavelets-based facial expression recognition using multi-layer perceptron, *IEEE International Conference on Automatic Face and Gesture Recognition*, 454–459. 1998
- [36] Buciu I., Kotropoulos C., Pitas I., ICA and Gabor representation for facial expression recognition, *IEEE International Conference on Image Processing (ICIP)*, 855–858. 2003.

- [37] Dubuisson S., Davoine F., Masson M., A solution for facial expression representation and recognition, *Signal Processing: Image Communication*, 17, 657–673. 2002
- [38] Shinohara Y., Otsu N., Facial expression recognition using fisher weight maps, *IEEE International Conference on Automatic Face and Gesture Recognition*, 499–504. 2004.
- [39] Kung H. W., Tu Y. H., Hsu C. T., Dual subspace nonnegative graph embedding for identity-independent expression recognition, *IEEE Transactions on Information Forensics and Security*, 10(3), 626-639, 2015.
- [40] Happy S. L., Routray A., Robust facial expression classification using shape and appearance features, *8th International Conference on Advances in Pattern Recognition (ICAPR)*, 1-5. 2015.
- [41] Shih F. Y., Chuang C., Wang P. S., Performance comparisons of facial expression recognition in JAFFE database, *International Journal of Pattern Recognition and Artificial Intelligence*, 22(3), 445-459, 2008.



Development of Pavement Maintenance Management System (PMMS) of Urban Road Network Using HDM-4 Model

Tanuj Chopra^{a*}, Manoranjan Parida^b, Naveen Kwatra^c, Jyoti Mandhani^d

^{a,c,d}Department of Civil Engineering, Thapar University, Patiala, India

^bDepartment of Civil Engineering, Indian Institute of Technology, Roorkee, India

*E-mail address: tchopra@thapar.edu

Received date: January 2017

Abstract

The aim of the study is to develop Pavement Maintenance Management System (PMMS) for four road sections of urban road network (Patiala, Punjab, India) using Highway Development and Management (HDM-4) model. The HDM-4 provides a deterministic approach in data input and process data of existing road condition, traffic volume and pavement composition to predict road deterioration as per the urban road conditions in terms of International Roughness Index (IRI) value. This study presents the use of HDM-4 model for the computation of optimum Maintenance and Rehabilitation (M&R) strategy for each road section and comparative study of scheduled and condition responsive M&R strategies. The results of present study will be useful for gaining better support for decision-makers for adequate and timely fund allocations for preservation of the urban road network.

Keywords: Pavement, management, maintenance, HDM-4, urban road, predict, road deterioration.

1. Introduction

Construction of road network involves substantial investment and therefore proper maintenance of these assets is of paramount importance. It is found that the actual available maintenance expenditure amount is much less than what is required for urban roads. It is a complex problem of matching of resources, time, materials, labour, equipment, funds, design and decision making. Therefore, maintenance and preservation of pavements should have a great national interest. Pavement Maintenance Management System (PMMS) consists of a comprehensive, coordinated, sets of activities associated with the planning, design, construction, maintenance and evaluation. Thus, PMMS can be used in directing and controlling maintenance resources for optimum benefits. Indeed, as a developing state, Punjab (India) pavements have some threats like increase rate of deterioration, rapid traffic growth, poor maintenance, overloading of vehicles, improper design and implementation, insufficient information for decision making and inefficient current traditional management system. Therefore, it is very essential to develop PMMS for the urban roads of Punjab and in this study, Patiala city has been taken to develop PMMS. Highway Development and Management Tool (HDM-4) was developed by World Bank to offer a powerful system for road maintenance and investment alternatives analysis, Archondo-Caallao [4]. HDM-4 analytical framework is based on the concept of pavement life cycle analysis. This is applied to predict road deterioration effects, work effect, user effect *etc.* Many researchers are working on the development of PMMS and effect of road surface deformations (Aydin and Topal [5], Ben-Edigbe [7], Ben-Edigbe and Ferguson [6], Ghasemlou et al. [9], Kerali et al.



[16], Pienaar et al. [26], Aggarwal et al. [1], Aggarwal et al. [2], Shah et al. [29], Girimath et al. [10], Gupta et al. [11]). Jain et al. [14] calibrated the HDM-4 pavement deterioration models for Indian National Highway Network located in the Uttar Pradesh and Uttaranchal states of India. They developed pavement performance prediction models for the major modes of distress, including cracking, raveling, potholes, and roughness on the basis of collected data. They also compared Indian deterioration models with HDM-4 deterioration models. Gupta et al. [11] determined the remaining service life of three road sections of Panchkula (Haryana). They concluded that from remaining service life values, all the selected road sections (in their study) would become candidates for reconstruction within 4 to 6 years without any maintenance work assigned during analysis period. Aggarwal et al. [3] developed PMMS for five Indian National Highway network using HDM-4 model; five National Highways, all were within the boundaries of Dehradun & Haridwar districts of Uttarakhand state and Saharanpur & Muzaffarpur districts of Uttar Pradesh state, comprising of total length of 310 km. Naidu et al. [24] developed maintenance management plan based on economics of life cycle costs using HDM-4 and he selected Inner Ring Road of New Delhi in his study. Dattatreya et al. [8] carried out a study on primary roads of Bangalore Metropolitan Development Authority Area. On the basis of their study, the requirements for the first stage road improvement program were worked out, consisting of strengthening and resurfacing of pavements, improvements in the drainage system and sidewalks and adopting measures to prevent early damages to pavements due to the leakage of water from pipes underneath the pavements and cutting of pavements across the roads at frequent intervals to take the service lines. Reddy et al. [28] developed a method of allocation of maintenance and rehabilitation costs based on the volume of commercial vehicles duly considering the load carried by them and the performance of pavements. They determined the cost allocation strategy for optimum maintenance and strengthening considering the yearly increase in vehicle operation cost due to the cumulative traffic loading during the analysis period. Reddy and Veeraragavan [27] developed a simple priority-ranking module that provided a systematic procedure to prioritize road pavement sections for maintenance depending upon the budget constraints. In their module, pavement sections under the jurisdiction of a highway agency were prioritized based on an overall pavement performance index derived from a combination of pavement surface distresses, traffic information and expert opinion. Jain et al. [15] developed optimum maintenance and rehabilitation strategy for multilane national highways by using programme analysis component of HDM-4 software. They had selected one expressway (from Noida to Greater Noida) divided into five sub-sections and one National Highway (NH-24, Ghaziabad-Hapur) divided into eight sub-sections. They concluded that M&R strategy which had higher NPV/CAP ratio was considered as optimum for the road section. On the basis of the economic analysis summary, they selected '25 mm SDBC Reseal and 40 mm BC overlay' for Expressway sections and for NH- 24 sections 'Thick Overlay of 40 mm BC' as the optimum M&R strategy having the maximum NPV/Cost among other alternatives.

The literature of PMMS for Indian road conditions revealed that there is no any PMMS developed for Indian urban roads and all the related studies of PMMS have been done for high category roads like national highways and expressways. The aims of the present study are to develop PMMS for urban road network of Patiala (Punjab, India) using HDM-4 model to determine optimum Maintenance and Rehabilitation (M&R) strategy for road sections of Patiala city using Project Analysis in HDM-4 model, prioritize Patiala city road sections based on optimum M&R strategy and to perform the comparative analysis of scheduled and condition responsive M&R strategies. The analysis period of 12 years (2017-2028) and for optimum M&R strategy Net Present Value (NPV)/Cost ratio have been taken.

2. Materials and Methods

2.1 Selection of Urban Road Sections

Patiala city (Punjab, India) has urban road network comprising of 52 road sections. The whole road network comes under the jurisdiction of Punjab Roads and Bridges Development Board (PR & BDB). In the present study, four road sections of Patiala each comprise of one km stretch have been selected and details of selected road sections of city have been shown in Table 1.

2.2 Data Collection and Analysis

Primary data for PMMS include pavement condition ratings, costs, roadway construction and maintenance history as well as traffic loading. To identify and evaluate pavement conditions and determine the causes of deterioration, a pavement evaluation system should be developed that is rapid, economical and easily repeatable. For this, pavement condition data has been collected periodically to document the changes of pavement condition.

The process of data collection was classified under following four categories:

- Road Network Data
- Traffic Volume and Vehicle Composition Data
- Maintenance and Rehabilitation (M&R) Works Data
- Road User Cost (RUC) Data

Road Network data refer to inventory data, pavement history data, and pavement condition data *etc.* Vehicle Fleet data include representation of vehicles with their basic characteristics. Maintenance and Rehabilitation Works data refer to details of maintenance activities for the road section. Costs data include road use cost data and data of cost of maintenance works.

Table 1. Details of selected road sections of Patiala city

Section ID	Section Name	Description	Section Length (Km)	Road Properties	Classification of Road
PR-01	Bhadson Road	From Central Jail to Sarabha Nagar	1.00	Two-Lane Wide Road	Collector Street
PR-02	Bhupinder Road	From Thapar University to Sahni's Bakery	1.00	Four-Lane divided Road	Collector Street
PR-03	Passey Road	From Thapar University to Charan Bagh	1.00	Narrow Two-Lane Road	Collector Street
PR-04	Ghuman Road	From Passey Road to Civil Lines	1.00	Two-Lane Standard Road	Local Street

2.2.1 Road Network Data

2.2.1.1 Road Inventory Data

Road inventory data collection consists of road length (m), lane width (m), shoulder width (m), geometries of road sections, traffic flow pattern, design speed (km/h), flow direction and climate zone. Road sections have been visually inspected to get relevant information. Details of road section inventory data has been presented in Table 2(a) and Table 2(b).

Table 2(a). Details of Inventory Data - 1

Section ID	Section Length (km)	Lane width (m)	Shoulder Width (m)
PR-01	1.00	8.4	1.4
PR-02	1.00	6.7	1.9
PR-03	1.00	6.5	1.6
PR-04	1.00	7.2	1.9

2.2.1.2 Pavement History Data

Pavement history data (type of pavement, year of last construction, surfacing and maintenance) has been collected from Public Works Department (PWD) office and Municipal Corporation of Patiala records from the year 2011 and 2015, Government of Punjab [17]. Details of pavement history data of road are presented in Table 3.

Table 2(b). Details of Inventory Data - 2

Section ID	Traffic Flow Pattern	Flow Direction	Design Speed (km/hr)	Climate Zone	Drainage condition
PR-01	Inter-Urban	Two-way	50	North India Plain	Good
PR-02	Inter-Urban	Two-way	50	North India Plain	Fair
PR-03	Inter-Urban	Two-way	50	North India Plain	Excellent
PR-04	Inter-Urban	Two-way	30	North India Plain	Poor

Table 3. Pavement history data

Section ID	Surfacing Material Type	Current Surface Thickness (mm)	Previous Surface Thickness (mm)	Last Construction Year	Last Rehabilitation Year	Last Surfacing Year	Last Preventive Treatment Year
PR-01	Bituminous Concrete (BC)	75	50	2003	2008	2013	2014
PR-02		75	50	2003	2009	2013	2014
PR-03		75	50	2004	2010	2014	2014
PR-04		75	50	2004	2009	2012	2012

2.2.1.3 Functional and Structural Evaluation of Road Pavements

The functional evaluation like roughness measurement survey has been conducted to assess the riding comfort and safety over the pavement section as experienced by road users. Road roughness refers to surface irregularities in the longitudinal direction and has been measured with fifth wheel bump integrator or simply known as 'Roughometer'. The equipment has been towed by pick-up and operated with speed of 30 kmph and shown in Figure 1. Accumulated bumps (in cms) has been noted down corresponding to length travelled (in km).

$$\text{Unevenness Index (UI)} = \text{Bumps in cm} / \text{Length travelled in km} \quad (1)$$

UI value has been converted into International Roughness Index (IRI in m/km) by using the following equation given by Odoki and Kerali [25]:

$$IRI = \left(\frac{1}{630} \times UI \right)^{1/1.12} \quad (2)$$

The structural evaluation has been carried out to assess the pavement's structural ability to receive wheel loads plying over it using rebound deflection measurements with the help of 'Benkelman Beam Deflection (BB_{def})Test' as shown in Figure 2. The test was conducted as per IRC: 81-1997 guidelines [12]. The Adjusted Structural Number (SNP) was calculated from deflection values by using the following equation given by Odoki and Kerali [25] and Table 4 presents the functional and structural evaluation data and Table 5 presents calibration factors for HDM-4 deterioration models.

For granular base courses

$$BB_{def} = 6.5 * (SNP)^{-1.6} \quad (3)$$

For bituminous base courses

$$BB_{def} = 3.5 * (SNP)^{-1.6} \quad (4)$$



Fig. 1. Bump integrator test (Roughness test)

Table 4. Functional and structural evaluation data

Section ID	Condition Year	Roughness, IRI (m/km)	Benkelman Beam Deflection (mm)	Adjusted Structural Number, (SNP)
PR-01	2016	1.99	0.43	5.46
PR-02		2.25	0.48	5.09
PR-03		2.16	0.44	5.38
PR-04		3.85	0.51	4.91

Table 5. Calibration factors for HDM-4 deterioration models

Model Description	Average Calibration Factor
Cracking Initiation Model	0.43
Cracking Progression Model	1.25
Ravelling Initiation Model	0.37
Ravelling Progression Model	0.52
Pothole Initiation Model	0.45
Pothole Progression Model	0.95
Roughness Progression Model	0.85
Rutting Progression Model	1.00

Aggarwal et al. [1] proposed the calibration factor is equal to 0.85 for National Highway Network when SNP range was of 3.0 - 5.3. It can be observed from Table 4 that SNP is in the range of 4.91 - 5.46 for present study, therefore the same calibration factor has been taken here. For pavement material evaluation, test pits of size 60 cm × 60 cm have been dug up for all the selected road sections to get information such as crust layer's thickness, California Bearing Ratio (CBR) of sub-grade soil and 'Atterberg Limits'. After taking the samples, laboratory tests such as light compaction test, CBR test, 'Atterberg Limits' test have been conducted on the collected soil. Table 6 presents the results of laboratory test on collected soil samples for selected road sections.



Fig. 2. Benkelman beam deflection test

Table 6. Laboratory test results of collected soil sample for all roads sections

Section ID	Optimum Moisture Content (OMC in %)	Atterberg Limit (%)			CBR (%) on Soaked sample
		Liquid Limit	Plastic Limit	Plasticity Index	
PR-01	12.4	19	15	4	5.2
PR-02	11.7	17	14	3	5.6
PR-03	13.8	22	16	6	4.5
PR-04	14.2	24	17	7	4.3

2.3 Traffic Volume and Vehicle Composition Data

Traffic volume counts are conducted manually for 72 hours consecutively by engaging adequate number of enumerators in individual road section. In the present study, traffic volume data and vehicular composition data have been collected from Municipal Corporation, Patiala. Annual Average Daily Traffic (AADT) for each section has been calculated by summing up the products of number of individual vehicle and its Passenger Car Space Equivalent (PCSE) factor. Table 7 presents the traffic volume of each section. Patiala road traffic comprises of both Motorized (MT) and Non-Motorized (NMT) vehicles. Percentage vehicle composition and Annual growth rate of vehicle for each road section has been provided in Table 8.

Table 7. Average Daily Traffic (AADT) data for road sections

Section ID	Motorized AADT (in PCSE)	Non-Motorized AADT	AADT year	Traffic Volume
PR-01	14,232	2,019	2016	High
PR-02	16,550	3,320	2016	High
PR-03	11,856	2,247	2016	High
PR-04	6,120	1,885	2016	Medium

Table 8. Vehicular composition and annual growth rate

Vehicle Type	Composition of Traffic Flow (%)								Annual Average Growth Rate (%)
	PR-01		PR-02		PR-03		PR-04		
	MT	NMT	MT	NMT	MT	NMT	MT	NMT	
Car/Jeep/Van	29.8	-	32.4	-	35.4	-	33.3	-	8.5
Mini Bus	3.90	-	0.60	-	0.60	-	-	-	3.7
Bus	3.60	-	0.80	-	0.80	-	-	-	4.0
Two Wheeler	39.8	-	43.9	-	41.0	-	49.1	-	4.2
Mini Truck	2.10	-	1.50	-	1.50	-	1.50	-	12.5
Truck (Medium)	3.40	-	0.80	-	-	-	-	-	5.0
Tractor/ Trolley	2.60	-	1.50	-	1.50	-	1.50	-	5.9
Auto Rickshaw	14.8	-	18.5	-	19.2	-	14.6	-	5.4
Cycle	-	46	-	49	-	56	-	60	3.4
Man-Driven Rickshaw	-	52	-	50	-	43	-	39	3.4
Cart	-	2	-	1	-	1	-	1	3.4
Total	100	100	100	100	100	100	100	100	

2.4 Maintenance and Rehabilitation Works Data

Maintenance serviceability levels for urban roads are suggested by Ministry of Road Transport and Highways (MORT&H) [23]. The suggested serviceability levels and the limiting levels of surface defects based on measurement of roughness, cracking, rutting *etc.* as per, (MORT&H, [23]), are given in Table 9.

Table 9. Maintenance serviceability levels for urban roads

S. No.	Serviceability Indicator	Serviceability Levels		
		Arterial Roads	Sub-Arterial Roads	Other Roads
1.	Roughness by Bump Integrator (max. permissible) Equivalent IRI (Odaki and Kerali, 2000)	2000 mm/km	3000 mm/km 4.0 m/km	4000 mm/km 5.2 m/km
2.	Potholes per km (max. number)	Nil	2-3	4-8
3.	Cracking and patching area (max. permissible)	5 percent	10 percent	10-15 percent
4.	Rutting - 20 mm (max. permissible)	5mm	5-10 mm	10-20 mm
5.	Skid number (min. desirable)	50 SN	40 SN	35 SN

For the present study, maintenance standard has been formed with basic design details and intervention criteria. The maintenance work standard for all road sections for reconstruction is condition responsive work *i.e.*, 200mm wet mix macadam, 75mm dense bituminous macadam and 40mm bituminous concrete with the intervention criteria of 'roughness ≥ 8 IRI'.

2.5 Cost Data of M&R Works

For the present study, the costs specified for urban roads in MORT&H, [19] is applicable. The cost (given in MORT&H, [19]) is relevant for the base year 1999-2000 and to include the effect of inflation, these costs are necessitated to be updated for application in consequent years. This has been made possible by provision of a mathematical model for annual updation of costs by linking labour component of the costs with Consumer Price Index (CPI), material component with Wholesale Price Index (WPI) and machinery component with average price of fuel (MORT&H, [19]).

$$\text{Percentage Increase in cost} = \left(\frac{F_L(I_1 - I_0)}{I_0} + \frac{F_M(W_1 - W_0)}{W_0} + \frac{F_F(F_1 - F_0)}{F_0} \right) * 100 \quad (5)$$

Where, F_L , F_M and F_F are the labour component, material component and machinery component of the cost, respectively. I_1 , W_1 and F_1 are the annual average CPI, WPI and fuel price, respectively, for the stated year (2015-16 in the present study) and I_0 , W_0 and F_0 are the annual average CPI, WPI and fuel price, respectively, for the base year 1999-2000. The percentage increase in cost for the year 2015-16 over the base year costs for routine maintenance is 125.26% and periodic maintenance is 205.40%. Table 10 presents updated economic cost data of M& R works for year 2016.

Table 10. Updated economic cost data of M&R works for year 2016

S. No.	Type of M&R Work	Cost per sq. m of Surface Area, Rs(\$)
Routine Maintenance		
1.	Crack Sealing (All Cracks)	66.4(0.99)
2.	Pothole Patching	84.7(1.27)
3.	Patch Repair	84.7(1.27)
4.	Rutting and Undulation Repair	117.7(1.76)
5.	Tack Coat	13.5(0.21)
6.	Liquid Seal Coat	68.8(1.03)
Periodic Maintenance		
1.	Single Bituminous Surface Dressing (SBSD)	178.5(2.67)
2.	Double Bituminous Surface Dressing (DBSD)	282.7(4.23)
3.	Premix Carpet (20mm PC)	223.2(3.34)
4.	Mix Seal Surfacing (20 mm MSS)	230.6(3.45)
5.	Semi Dense Bituminous Concrete (25mm SDBC)	208.3(3.12)
6.	Bituminous Concrete (25mm BC)	230.6(3.45)
7.	Bituminous Concrete (40mm BC)	369.0(5.52)
8.	Bituminous Macadam (50mm BM)	370.5(5.54)
9.	Dense Bituminous Macadam (75mm DBM)	614.5(9.19)
10.	Mill 90mm and Replace with (BM 50mm + BC 40mm)	739.4(11.20)
11.	200 mm Wet Mix Macadam + 75 mm Dense Bituminous Macadam + 40mm Bituminous Concrete	1429.8(21.38)

2.6 Road User Cost (RUC) Data

Road User Cost (RUC) consists of three components *i.e.*, Vehicle Operating Costs (VOC), Travel Time Costs (TTC) and Accident Costs (AC). VOC is the dominating component in RUC. In present study, VOC component has been considered and has been calculated as per Clause 6.6 (Annexure C) and Clause 6.9 of IRC SP: 30, [13]. Table 11 shows vehicle operating cost data input per 1000 vehicles-km and economic cost (exclusive of tax) has been considered here.

2.7 Proposed M&R Alternatives

Four M&R alternatives have been proposed for this objective and given in Table 12 (keeping in mind the serviceability level of other roads).

2.8 Comparative Study of Scheduled and Condition responsive M&R Strategies

Comparison of adopting a scheduled type M&R strategy against a condition responsive M&R strategy for individual road section throughout the analysis period has been done. Analysis period was taken as 12 years, start year with 2017 and PR-01 has been selected for Patiala city urban road network. Discount rate of 12 % has been taken for present study.

Table 11. Vehicle operating costs data input per 1,000 vehicle-km

Parameter	Two-wheeler	Car/Jeep/Van	Bus (Medium)	Mini Bus	Trucks (Medium)	Mini Truck	Tractor/Trolley
Cost of Fuel (Rs(\$)/litre)	620(9.27)	1400(20.93)	5530(82.6)	4570(68.4)	5730(85.7)	4570(68.32)	4570(68.32)
Cost of Lubricants (Rs(\$)/litre)	4(0.06)	16(0.24)	13(0.19)	13(0.19)	20(0.30)	13(0.19)	13(0.19)
Maintenance Labour (Rs(\$)/hr)	4.06(0.06)	6.40(0.10)	25.5(0.38)	9.22(0.14)	28.27(0.42)	9.22(0.14)	9.22(0.14)
Crew Wages (Rs(\$)/hr)	-	-	1.17(0.02)	4.08(0.06)	2.20(0.03)	4.08(0.06)	4.08(0.06)
Annual Overhead	0.25(0.01)	0.91(0.01)	0.84(0.01)	4.67(0.07)	2.60(0.04)	4.67(0.07)	4.67(0.07)
Annual Interest (in %)	8	8	8	8	8	8	8

Table 12. Proposed M&R alternatives

M&R Strategy	Works Standard	Description of Work	Intervention Level
Base Alternative	Routine	Crack Sealing	Scheduled annually
		Patching	Scheduled annually
Alternative 1	Resealing + Thin Overlay	Provide 25 mm DBSD	Total damage area > 8% of total area
		Provide 25 mm BC	Roughness ≥ 4 , ≤ 5.8 IRI
Alternative 2	Thick Overlay	Provide 40 mm BC	Roughness ≥ 5.8 , ≤ 8 IRI
Alternative 3	Reconstruction	Provide (200 mm Wet Mix Macadam + 75 mm Dense Bituminous Macadam + 40mm Bituminous Concrete)	Roughness ≥ 8 IRI

2.8.1 Proposed M&R Alternatives

The Scheduled M&R strategy has been chosen as per the current maintenance norms provided in MORT&H, [19], where as the Condition Responsive M&R strategy has been selected as per the serviceability levels up to which the respective pavement section is to be maintained (Guidelines for Maintenance of Primary, Secondary and Urban Roads, MORT&H, [22]). Proposed M&R Alternatives have been presented in Table 13.

3. Results and Discussions

3.1 Determination of Optimum M&R Strategy for All the Selected Road Sections

Economic analysis for the selected roads has been done with discount of 12% (Clause 7.8, IRC: SP: 30, [13]). As a result of this analysis, the road pavement deterioration/works reports and M&R works reports have been generated corresponding to each M&R alternative

considered. The Roughness progression graphs of all the four alternatives for all the four road sections are shown individually from Figure 3 to Figure 6. The roughness progression has been traced to know whether the works have been correctly triggered according to the specified intervention criteria or not.

Table 13. Proposed M&R alternatives for project analysis of PR-04

M&R Alternative	M&R Work		Work Item	Intervention Criteria
Routine Maintenance	Routine		Patching	Scheduled Annually
			Crack Sealing	Scheduled Annually
Scheduled Overlay	Bituminous (BC) 25 mm Thick	Concrete	Provide BC 25 mm	Scheduled every Five years
Condition Responsive Overlay	Bituminous (BC) 25 mm Thick	Concrete	Provide BC 25 mm	Roughness \geq 4.0 m/km IRI

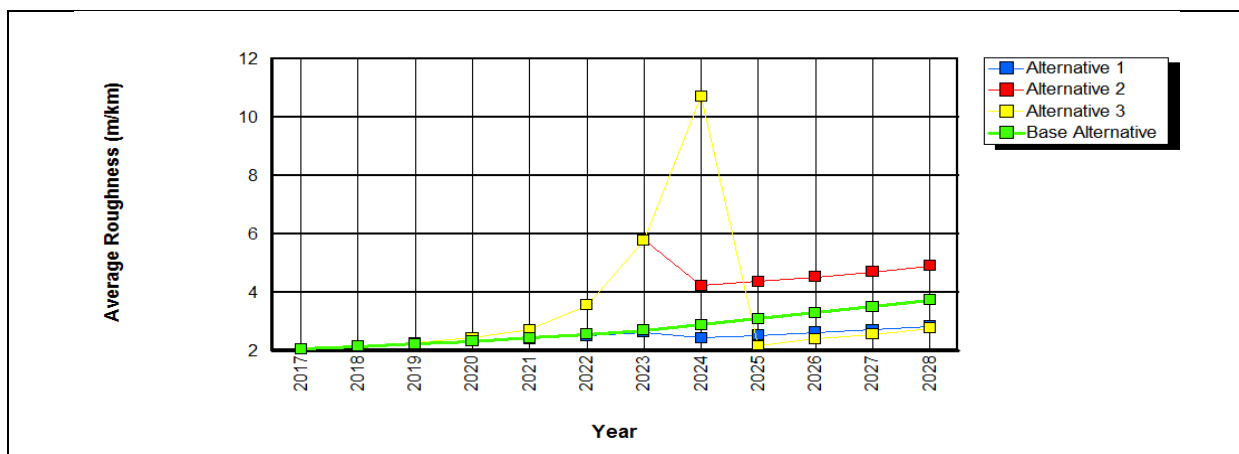


Fig. 3. Roughness progressions under all alternatives for PR-01

Roughness is considered to be the most useful indicator of the pavement deterioration, or average condition of the pavement section at any given point of time. The effect of the works to be carried out under each M & R strategy, on average roughness of the selected pavement sections has been shown in Figure 3 to Figure 6. The progression of roughness can be tracked to check that the works have correctly triggered according to the specified intervention criteria; as for road section PR-04 (shown in Figure 6), 'reconstruction' has been triggered under Alternative 3 at the end of the year 2022 (peak value in PR-04 with Alternative 3 graph line) for the road section PR-04, when the average roughness value for the pavement section has crossed the intervention level of 8 m/km IRI. Similarly, Alternative 2 of 'overlay' has been triggered, when roughness value exceeds 5.8 m/km IRI, in the year 2022. This application of overlay has been indicated by drop in roughness value to 4.0 m/km.

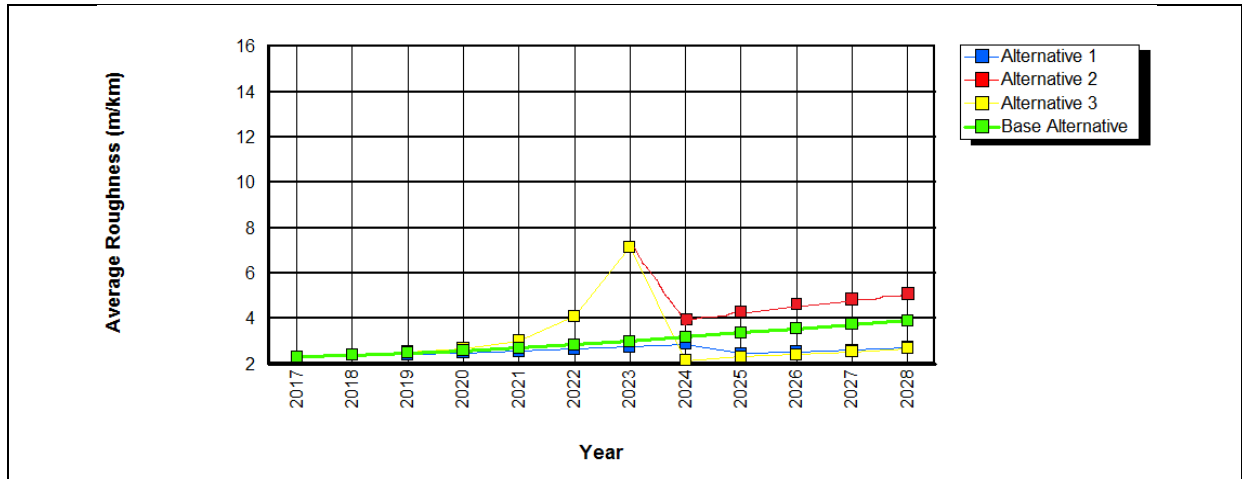


Fig. 4. Roughness progressions under all alternatives for PR-02

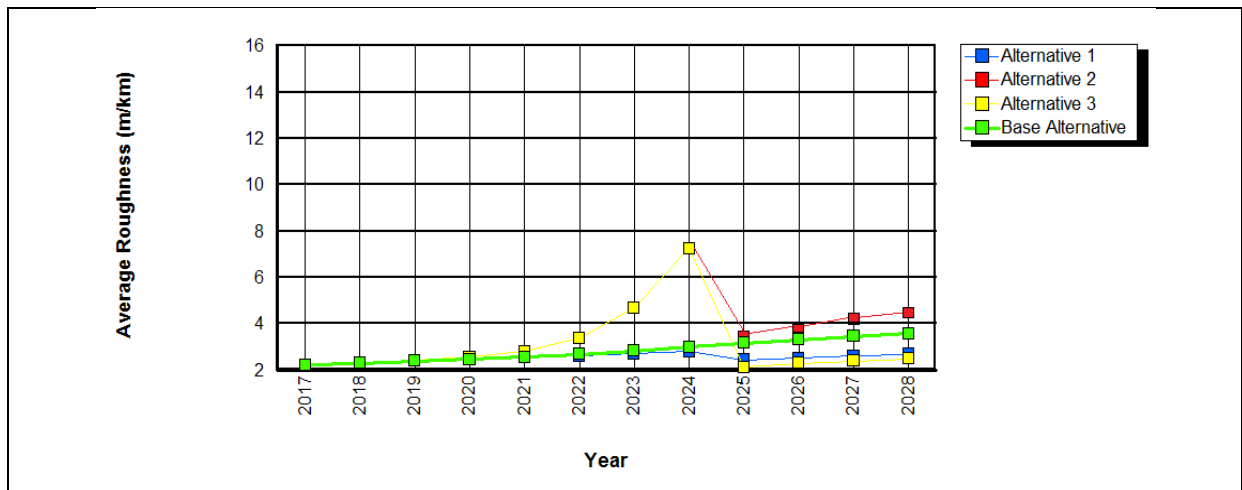


Fig. 5. Roughness progressions under all alternatives for PR-03

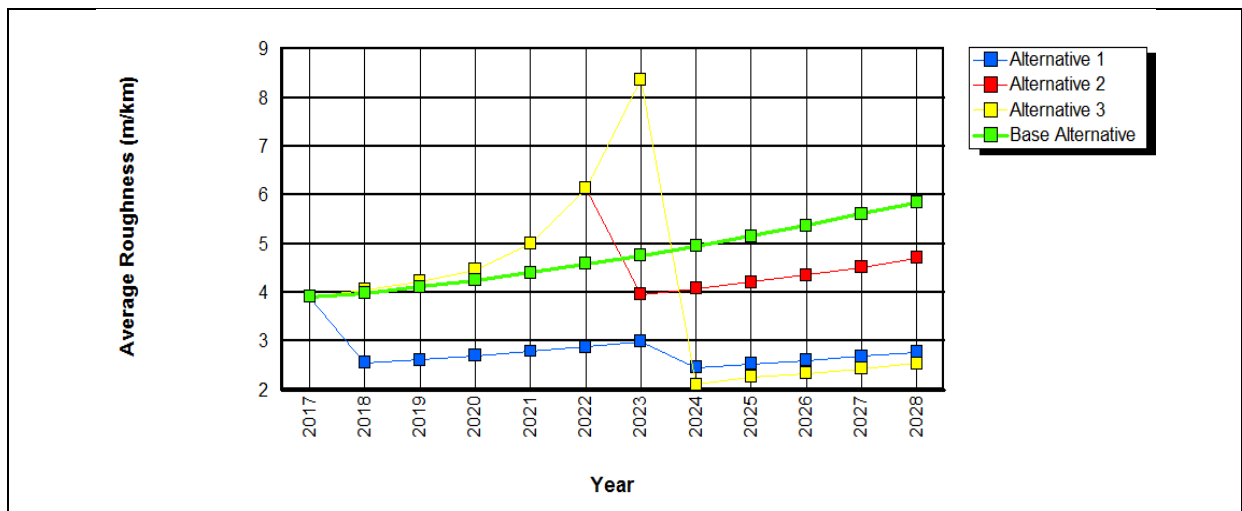


Fig. 6. Roughness progressions under all alternatives for PR-04

The year-wise summary report of each alternative for all the road sections have been mentioned in Table 14 to Table 16. This report has given the description of works that would be implemented in each year of the analysis period (2017-2028), under each M&R strategy. Year-wise summary reports for all the four road sections corresponding to each alternative

presented in Table 15 to Table 16. In Table 16, Alternative 1 *i.e.*, 'Resealing + thin overlay' will be required in year 2018, 2023 and 2028 for PR-01; in year 2018 and 2024 for PR-02; in year 2017 for PR-03 and in year 2023 for PR-04 during the analysis period of 12 years (2017 - 2028). Alternative 2 *i.e.*, '40mm BC' will be applied in year 2023 for section PR-01 and PR-02, in year 2024 for PR-03 and in year 2022 for section PR-04 as shown in Table 15. Alternative 3 *i.e.*, 'reconstruction' will be applied in year 2023 for PR-02 and PR-04 and in year 2024 for PR-01 and PR-03 as shown in Table 16. Selection of optimum M&R strategy by economic analysis has based on any of the economic indicators *i.e.*, Net Present Value/Cost (NPV/Cost) Ratio, Internal Rate of Return (IRR) or Net Benefits. In the present study, economic indicator NPV/Cost ratio has been considered for selection of optimum M&R strategy for all the road sections. The summaries of economic analysis for all the road sections are shown in Table 17 to Table 20.

Table 14. Year-wise summary report of Alternative 1 for all road sections

Year	Alternative 1			
	PR-01	PR-02	PR-03	PR-04
2017	****	****	****	25 mm DBSD
2018	25 mm DBSD	25 mm DBSD	25 mm DBSD	****
2023	25 mm DBSD	****	****	25 mm DBSD
2024	****	25 mm DBSD	25 mm DBSD	****
2028	25 mm DBSD	****	****	****

**** means no M&R work assigned in the certain year

Table 15. Year-wise summary report of Alternative 2 for all road sections

Year	Alternative 2			
	PR-01	PR-02	PR-03	PR-04
2022	****	****	****	40 mm BC
2023	40 mm BC	40 mm BC	****	****
2024	****	****	40 mm BC	****

Table 16. Year-wise summary report of Alternative 3 for all road sections

Year	Alternative 3			
	PR-01	PR-02	PR-03	PR-04
2023	****	200 mm WMM +75 mm DBM + 40 mm BC	****	200 mm WMM +75 mm DBM + 40 mm BC
2024	200 mm WMM +75 mm DBM + 40 mm BC	****	200 mm WMM +75 mm DBM + 40 mm BC	****

Table 17. Summary of economic analysis for PR-01

Alternative	Present value of Road Agency Costs, Rs(\$) in Millions	Increase in Agency Cost, Rs(\$) in Millions	Decrease in Road User Costs, Rs(\$) in Millions	Net Present Value, Rs(\$) in Millions	NPV/Cost Ratio	Internal Rate of Return
Base	0.154(2264)	0.000	0.000	0.000	0.000	0.000
Alternative 1	3.996(58764)	3.842(56500)	26.092(383705)	22.250(327205)	5.568	51.5
Alternative 2	1.570(23088)	1.416(20823)	2.918(42911)	1.502(22088)	0.957	21.03
Alternative 3	5.434(79911)	5.279(77632)	8.186(120382)	2.907(42750)	0.535	16.8

Table 18. Summary of economic analysis for PR-02

Alternative	Present value of Road Agency Costs, Rs(\$) in Millions	Increase in Agency Cost, Rs(\$) in Millions	Decrease in Road User Costs, Rs(\$) in Millions	Net Present Value, Rs(\$) in Millions	NPV/Cost Ratio	Internal Rate of Return
Base Alternative	0.250(3676)	0.000	0.000	0.000	0.000	0.000
Alternative 1	5.083(74750)	4.834(71088)	22.358(328794)	17.525(257720)	3.448	46.1
Alternative 2	4.945(72720)	4.698(69088)	7.344(108000)	2.646(38911)	0.535	16.8
Alternative 3	9.708(142764)	9.458(139088)	15.389(226308)	5.931(87220)	0.611	17.2

Table 19. Summary of economic analysis for PR-03

Alternative	Present value of Road Agency Costs, Rs(\$) in Millions	Increase in Agency Cost, Rs(\$) in Millions	Decrease in Road User Costs, Rs(\$) in Millions	Net Present Value, Rs(\$) in Millions	NPV/Cost Ratio	Internal Rate of Return
Base Alternative	0.120(1764)	0.000	0.000	0.000	0.000	0.000
Alternative 1	2.466(36264)	2.346(34500)	7.504(110352)	5.158(75852)	2.092	33.0
Alternative 2	2.399(35279)	2.279(33514)	3.452(50764)	1.173(17250)	0.489	14.7
Alternative 3	4.205(61838)	4.085(60073)	6.216(91411)	2.131(31338)	0.507	15.3

Table 20. Summary of economic analysis for PR-04

Alternative	Present value of Road Agency Costs Rs(\$) in Millions	Increase in Agency Cost, Rs(\$) in Millions	Decrease in Road User Costs, Rs(\$) in Millions	Net Present Value, Rs(\$) in Millions	NPV/Cost Ratio	Internal Rate of Return
Base Alternative	0.088(1294)	0.000	0.000	0.000	0.000	0.000
Alternative 1	3.059(44985)	2.972(43705)	29.157(428779)	26.186(385088)	8.560	129.6
Alternative 2	1.508(22176)	1.420(20882)	3.513(51661)	2.093(30779)	1.389	22.2
Alternative 3	5.216(76705)	5.129(75426)	8.977(132014)	3.848(56588)	0.738	20.4

On the basis of economic analysis of each alternative for all the road sections, optimum M&R strategy has been selected. The alternative which has higher NPV/Cost ratio for any road section compared to the other predefined alternatives, is selected as optimum M&R strategy for that section. Table 21 shows the optimum M&R alternative selected for each road section.

Table 21. Optimum M&R Alternative for each road section

Section ID	Section Name	Optimum M&R Strategy
PR-01	Bhadson Road	Alternative 1
PR-02	Bhupinder Road	Alternative 1
PR-03	Passey Road	Alternative 1
PR-04	Ghuman Road	Alternative 1

3.2 Prioritization of Road Sections Based on Optimum M&R Strategy

Based on optimum M&R strategy of the road sections, prioritization of all the road sections has been done. Higher the NPV/Cost ratio of optimum M&R strategy of the road section, higher will be the prioritization ranking of that road. Table 22 shows the prioritization ranking of road sections based on optimum M&R strategy.

Table 22. Prioritization ranking of road section

Section ID	Section Name	Optimum M&R Strategy	NPV/Cost Ratio	Prioritization Ranking
PR-04	Ghuman Road	Alternative 1	8.560	1
PR-01	Bhadson Road	Alternative 1	5.568	2
PR-02	Bhupinder Road	Alternative 1	3.448	3
PR-03	Passey Road	Alternative 1	2.092	4

3.3 Comparative Analysis of M&R Strategies

The Roughness progression graph of all the three alternatives for PR-01 has been shown in Figure 7. The roughness progression has been traced to know whether the works have been correctly triggered corresponding to the specified intervention criteria. In case of ‘Condition Responsive Overlay’ alternative, overlay work has been triggered as soon as the roughness value reaches 4 IRI. But in case of Scheduled overlay alternative, overlay work has been triggered in every five years, but roughness value of IRI is equal to 2.4 m/km or even less, which is well below the limiting value of IRI is equal to 4 m/km (serviceability level for other roads). The various work items resulting from the two M&R alternatives specified, as triggered by the respective intervention parameters and timings of their application are shown in Table 23. Total road costs for both M&R alternatives have been shown. The cost comparison of the two defined M&R alternatives clearly shows that in case of adopting Scheduled type M&R strategy, road agency will have to spend Rupees 5.811 millions on overlaying the road section three times throughout the period of 12 years. However, in case they adopt Condition Responsive type M&R strategy, the agency may have to spend only Rupees 1.937 million on overlaying the road section one time through the same period. In adopting the Scheduled type M&R strategy, the road agency will have to spend about 3 times more than the cost of Condition Responsive M&R strategy. Hence, there will be huge net saving in cost in case of Condition Responsive type M&R strategy as compared to scheduled type M&R strategy. The Condition Responsive M&R strategy can hence be affirmed as cost effective M&R strategy.

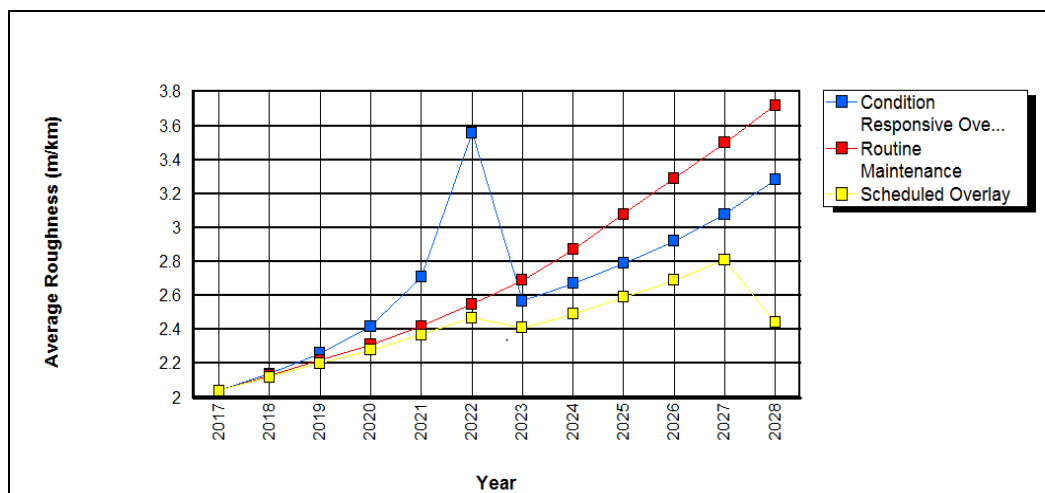


Fig. 7. Roughness progression under the three alternatives for PR-01

Table 23. Description of M&R works with total road agency costs

M&R Alternative	M&R Work	Applicable Years	Frequency of Application	Total Road Agency Costs in Million Rupees
Scheduled Overlay Condition	Bituminous Concrete 25 mm Thick	2017, 2022, 2027	3	5.811
Responsive Overlay	Bituminous Concrete 25 mm Thick	2022	1	1.937

4. Conclusions

- The optimum M&R strategy for all road section of Patiala city road network has been determined successfully based on highest NPV/cost ratio using HDM-4. Amongst a number of defined M&R strategies; Alternative 1 *i.e.*, ‘Resealing + Thin Overlay’ has been selected as optimum M&R strategy for all the road sections. Hence, the use of PMMM techniques can lead to a coordinated, cost-effective strategy for maintaining pavements.
- On the basis of optimum M&R strategy, prioritization of road sections for maintenance works has been successfully done for all the road sections. In case of constrained budget, maintenance of road sections could be done based on prioritization ranking of road sections *i.e.*, first preference will be given to PR-04, second to PR-01, third to PR-02 and last preference will be PR-03 for maintenance work. The HDM-4 model effectively prioritizes all the road sections for the present study. Since, prioritization is a decision making process, designers must use good models like HDM-4 before taking important decisions.
- Comparative study of Scheduled type and Condition Responsive type M&R strategies has been successfully carried out for Bhadson Road section. The cost comparison of the two defined M&R alternatives clearly show that in adopting the Scheduled type M&R strategy, the road agency will have to spend about 3 times higher than the cost of Condition Responsive M&R strategy. Condition Responsive M&R strategy is hence chosen as the cost effective M&R strategy.

References

- [1] Aggarwal, S., Jain, S.S and Parida, M., A critical appraisal of pavement management systems. *Journal of Indian Road Congress*, 63(2), 2002.
- [2] Aggarwal, S., Jain, S.S and Parida, M., Development of pavement management system for Indian national highway network. *Journal of Indian Road Congress*, 65(2), 271-326, 2004.
- [3] Aggarwal, S., Jain, S.S and Parida, M., Use of pavement management systems in Developing Countries, *Indian Highways*, 5 – 17, 2005.
- [4] Archondo-Callao, R., Allying the HDM-4 model to strategic planning of road works, *The World Bank Group*, Washington, D.C., 2008.
- [5] Aydin, M.M., Topal A., Effect of road surface deformations on lateral lane utilization and longitudinal driving behaviours, *Transport*, 31,192-201, 2016.
- [6] Ben-Edigbe, J., Ferguson, N., Extent of capacity loss resulting from pavement distress, *Proceedings of the Institution of Civil Engineers – Transport*, 158(1): 27–32, 2005.

- [7] Ben-Edigbe, J., Assessment of speed–flow–density functions under adverse pavement condition, *International Journal of Sustainable, Development and Planning*, 5(3), 238–252, 2010.
- [8] Dattatreya, J.K., Veeraragavan A., Murthy, K. and Justo, C.E.G., A suggested simplified system for pavement maintenance management of road network. *Journal of Indian Roads Congress*, 53(2), 217-273, 1992.
- [9] Ghasemlou, K., Aydin, M.M., Yıldırım, M.S., Karpuz, O. and İmamoğlu, C.T., Investigation the effect of road surface deformations on capacity of signalized intersections by using cell transmission model, *11th International Congress on Advances in Civil Engineering, Istanbul, Türkiye*, 1-10, 2014.
- [10] Girimath, S. B. and Fellow, P., Pavement management system for urban roads. *International Journal of Scientific and Development*, 2(3), 282–284, 2014.
- [11] Gupta, P. K., and Kumar, R., Development of optimum maintenance and rehabilitation strategies for urban bituminous concrete surfaced roads. *International Journal of Scientific and Technology Research*, 4(2), 56-66, 2015.
- [12] IRC: 81, Guidelines for strengthening of flexible road pavement using benkelman beam deflection technique. *Journal of Indian Roads Congress*, New Delhi, 1997.
- [13] IRC SP: 30, Manual on economic evaluation of highway projects in India. *Journal of Indian Roads Congress*, New Delhi, 2009.
- [14] Jain, S. S., Aggarwal, S., and Parida, M., HDM-4 pavement deterioration models for Indian national highway network. *Journal of Transportation Engineering*, 131(8), 623–631, 2005.
- [15] Jain, K., Jain, S. S., and Chauhan, M. S., Selection of Optimum Maintenance and Rehabilitation. *International Journal for Traffic and Transportation Engineering*, 3(3), 269–278, 2013.
- [16] Kerali, H. R., Henry, G. R., Odoki, J. B. and Stannard, E. E., HDM-4, Overview of HDM-4. *The World Road Association (PIARC)*, 2000.
- [17] Government of Punjab, Master Plan Patiala, *Department of town and country Planning Punjab*, 2011.
- [18] MORT&H, Report of the committee on norms for maintenance of roads in India. *Ministry of Road Transport & Highways*, Government of India, New Delhi, 2001a.
- [19] MORT&H, Road Development Plan Vision: 2021. *Ministry of road transport & highways*, Government of India, New Delhi, 2001b.
- [20] MORT&H, Updation of road user cost data. Final Report prepared by *Central Road Research Institute for Ministry of Road Transport & Highways*, Government of India, New Delhi, 2001c.
- [21] MORT&H, Specifications for maintenance works. *Ministry of Road Transport & Highways*, Government of India, New Delhi, 2001d.
- [22] MORT&H, Specifications for maintenance works. *Ministry of Road Transport & Highways*, Government of India, New Delhi, 2004.
- [23] MORT&H, Specifications for maintenance works. *Ministry of Road Transport & Highways*, Government of India, New Delhi, 2013.
- [24] Naidu, S.S., Nanda, P.K., Kalla, P., Sitaramanjaneyulu, K., Pavement maintenance management system for urban roads using software HDM-4 A Case Study. *Journal of Indian Roads Congress*, 66(3), 641– 669, 2005.
- [25] Odoki, J. B. and Kerali, H. R., Analytical framework and model descriptions. *The World Road Association (PIARC)* on behalf of the ISOHDM sponsors, 2013.
- [26] Pienaar, P. A., Visser, A. T. and Dlamini, L., A comparison of the HDM-4 with the HDM-III on a case study in Swaziland. *South African Transport Conference. South Africa*, 2000.

- [27] Reddy, B.B. and Veeraragavan, A., Priority ranking model for managing flexible pavement at management level, *Centre for Transportation Engineering*, Bangalore University, Bangalore, 378–394, 2001.
- [28] Reddy, B.B. and Veeraragavan, A., Priority ranking model for managing flexible pavements at network level, *Technical Paper Published in 62nd annual session of Indian Roads Congress(IRC)*, Kochi, India, 2002.
- [29] Shah, Y. U., Jain, S. S. and Parida, M., Evaluation of prioritization methods for effective pavement maintenance of urban roads. *International Journal of Pavement Engineering*, 15(3), 238–250, 2012.



Utilization of a New Methodology on Performance Measurements of Red Light Violations Detection Systems

Metin Mutlu Aydin ^a, Sevil Kofteci ^{b*}, Kadir Akgol ^c and Mehmet Sinan Yildirim ^d

^{a,b,c} Akdeniz University, Civil Engineering Department, Antalya, TURKEY

^d Celal Bayar University, Civil Engineering Department, Manisa, TURKEY

*E-mail address: skofteci@akdeniz.edu.tr

Received date: February 2017

Abstract

In recent years, intelligent transportation systems are under a continuous development which are the direct integration of the technology and traffic engineering aspects. These systems are extensively used in order to prevent driving at high speeds and violations of the traffic rules at different road sections, signalized and unsignalized intersections. These systems have capabilities of detecting the instantaneous and average speeds of vehicles along a roadway section, and red light violations. By the help of these sophisticated systems, road and security authorities can successfully carry out criminal sanctions against non-compliant drivers combined with plate reader cameras. In Turkey, these systems are called Traffic Electronic Control System (TECS) and they are considered under different categories such as intelligent intersection systems, vehicle counting systems, safety strip violation detection systems, speed violation detection systems, speed corridors, red light violation detection systems and parking violation detection systems. Within the scope of this study, the performance of a red light violation system installed at the 4-leg signalized intersection at Antalya-Burdur highway entrance of Celtikci district belonging to the TECS was investigated by implementing a new proposed methodology. According to the performance analysis of the system, it was found that system has maximum 2 seconds error limit and its performance was found appropriate for all conditions (green to red, red to green, all green and all red). This study also demonstrated that the new measurement method accurately measures the performance of the system by examining all measurement possibilities.

Keywords: Traffic electronic monitoring systems, signalized intersection, red light violation detection, intelligent transportation systems.

1. Introduction

Traffic accidents at signalized and unsignalized intersections have an important percentage among the all traffic accidents in Turkey based on the official accident statistics [1, 2]. This phenomena can easily be provided based on the traffic accident statistics with the spatial distribution data for the last five years as shown in Table 1 [3-7].

Table 1. Statistics of traffic accidents and their spatial distribution in the last 5 years in Turkey [3-7]

Year	The Number of Total Accidents	Number of Accidents at Intersections (%)	Number of Accidents at Intersections caused by red light violation (%)
2011	1.228.928	110.803 (9.0%)	3184 (2.9%)
2012	1.296.634	130.360 (10.1%)	3517 (2.7%)
2013	1.207.354	161.306 (13.4%)	3137 (1.9%)
2014	1.199.010	168.512 (14.1%)	3445 (2.0%)
2015	1.313.359	1830.11 (13.9%)	3967 (2.2%)



When Table 1 is examined, it can be seen that the ratios of the traffic accidents at intersections have a fixed value over years and no significant decrease was observed. Many studies carried out around the world also indicated that the drivers are not disciplined in utilizing the lanes and speedy driving, red light violations were among the important problems affecting the traffic safety and increasing the road accidents [2, 8-10]. In their study, Coruh et al. [2] found that the fast rate of urbanization, along with increasing employment rates, places significant strain on have an important effect on traffic accidents for Turkey. Therefore, they suggested that Turkey needs to develop some countermeasures such as, well-designed road infrastructure networks across the country that is sustained over a long term. Also according to their study results, it was found that road-surveillance cameras strictly enforce speed limits and it was found that an increase in the number of red light traffic violations increases the number of accident counts significantly.

In recent years, intelligent transportation systems are under a continuous development which are the direct integration of the technology and traffic engineering aspects. These systems have capabilities of detecting the instantaneous and average speeds of vehicles along a roadway section, and red light violations. By the help of these sophisticated systems, road and security authorities can successfully carry out criminal sanctions against non-compliant drivers combined with plate reader cameras. One of the most applied places of these systems are signalized intersections where they are frequently used for detecting red light violations. The outcomes of the studies in many countries indicated that the vast majority of accidents that occurred at both signalized and unsignalized intersections were caused by the drivers who are not following the red light rule. To prevent the negative effect of red violations, red light violations detections systems are used in many countries (India, Turkey, USA, Iran, Brasil etc.) and in many intersection types (T, 4-leg, 3-leg, etc.) [11-15]. To examine and determine the effect of this system many studies were conducted by the researchers. For example, Baguley [16] observed that some drivers intentionally violate the red light and he reached the conclusion that to eliminate this problem, detection systems must be implemented. Yang and Najm [17] have found that these systems influence the behaviors of the drivers encountering the red lights, and especially they indicated that, warning plates placed at the intersections are helpful for taking the attention of the drivers. Yang and Najm [17] stated that, the average speed of the drivers passing during the red light state was 31.6 mph and they added that 94% of the drivers made the violations 2 seconds after the red light state initiated and 2.7% of these drivers made the red light violation after 2 to 5 seconds after the initialization of the red light state. They also indicated that the drivers who violated the red lights were often elderly drivers (1.5 times more than young drivers) probably resulted by the weakening of the driver's perception with the age. Lum and Wong [18] considered a "T" type intersection after installation of the red light violation system. They reported that red light violations were reduced to a value between 13.4 to 58.6 from 16 to 111.8 vehicles per day after the initialization of the system. In a similar study, Schattler et al. [19] investigated three intersections and stated that red light violations were reduced to 0 to 4.6 vehicles from 0 to 10.2 vehicles per hour with the installation of the red light violation detection systems. According to the Ruby and Hobeika [20], the installation of these systems reduced the red light violation cases to 0.17 to 7 vehicles per 10.000 cars from 2 to 11 vehicles. Fitzsimmons et al. [9] investigated the effects of these systems on the number of accidents that occurred at intersections. From the analyzes it was concluded that the total number of accidents at intersections was reduced by 44%, the rear-front collisions were reduced by 40% and non rear-front collisions were reduced by 90%. Considering these studies in literature, existing studies generally considered the effect of the red light violation detection system on violation numbers and accidents. Apart from that there is a serious concern in the literature about how to verify the accuracy of these systems (corresponding control methods) and how to determine the limit values or thresholds that drivers will not to be aggrieved.

Within the scope of this study, the application of these systems has been focused on the reliability of detection of the red light violations and how to test these systems in manner of detection validity and performance. Particularly, the performance of a red light violation system installed at the 4-leg signalized intersection at Antalya-Burdur highway entrance of Çeltikçi district belonging to the TECS was investigated by implementing a new proposed methodology.

2. Red Light Violation Detection Systems and Working Principles

In Turkey, Traffic Electronic Control Systems, covered by TECS, are considered under different categories such as intelligent intersection systems, vehicle counting systems, safety strip violation detection systems, speed violation detection systems, speed corridors, red light violation detection systems and parking violation detection systems. These systems were implemented for sustaining a safe traffic flow by detecting the traffic rule violations and penalize the corresponding drivers to influence the driver's respect against the rules. Red Light Violation Detection Systems (KITS) is one of the most used systems of TECS in practice. KITS are developed with the aim of preventing accidents caused by red light violations at signalized intersections, detecting the offender drivers and applying criminal sanctions (See Figure 1).



Fig.1. An example of a red light violation detection system (a) 3D design (b) real life application

The general characteristics of these systems can be summarized as follows [21-24]:

- System detects the traffic signal color by using a specialized detector device and receives the transmitted signal for evaluating the signal phase and the vehicle arrivals. All these parameters simultaneously evaluated together and reported to the recording unit so that the possibility of encountering an error is minimized.
- Violations are detected from backward-direction photographs that are taken afterwards the passage of a vehicle to provide the necessary evidence that the driver has violated the rules.
- The red color of the traffic signal transmitter is clearly displayed in the infringement picture.
- System can receive uninterrupted video recording for 24 hours.
- The authenticity of the images is guaranteed with the digital signature method for legal proof of the infringement images.

- The digital camera technology used in the systems has the ability to take high-resolution serial images, multiple-lane violation detection feature, and the ability to detect all the violations that occur at the same time.

These systems use virtual loop creation and image analysis methods on the road to detect vehicles passing through red light. The system automatically identifies the plates of the infringing vehicles and transfers the information to the management software. The software can detect multiple violating vehicles at the same time thanks to the video analysis techniques and transmit all the images to the authorities belonging to the violation moment, before and after the violation. The software has the capability of detecting and reporting the drivers to the operator and the ticketing is performed automatically with the approval of the operator.

3. General Information about the Examined Intersection

Within the scope of the study, Red Light Violation Detection Systems applied to 4-leg signalized intersection located at "37.533823 30.482611" coordinates on the Antalya-Burdur highway were examined (Figure 2).



Fig.2. The corresponding intersection on the Antalya-Burdur highway Çeltikçi region, which is investigated for the red light violation detection system.

The investigation procedure was performed during the day light hours (06:30 am – 09:00 am) Different views from the investigated intersection is shown in Figure 3.



Fig.3. Different views from the investigated intersection.

There are two important cases to be aware of when checking the reliability of the red light violation detection system. One of the case of the failure is that the system may ticket a vehicle which is not passing at the red light state and the second one is that the system may miss a vehicle which passes at the red light state. In the analyses, both of the case were considered by the investigation team by taking video recordings based on different vehicle approaching scenarios. For this eight different scenarios were prepared. The prepared study paper was shown in the Figure 4. According to these scenarios, the cases below were investigated.

- For the transition period from the red to the green and green to red light states, the passage of the vehicle 2-3 seconds after the red, yellow and green states were initialized.

The 2 to 3 delay seconds was considered to reflect the behaviors of the drivers under the influence of the dilemma zone who prefer to pass instead of stopping at the intersection. By this way, a safety factor methodology was added to the analysis results.

RED LIGHT VIOLATION DETECTION SYSTEM TEST WORKSHEET

Start Time :
End Time :

<input type="checkbox"/> R-Y-G	<input type="checkbox"/> R-Y-G
<input type="checkbox"/> R-Y-G-2	<input type="checkbox"/> R-Y-G-2
<input type="checkbox"/> R-G-2	<input type="checkbox"/> R-G-2
<input type="checkbox"/> Y-G-2	<input type="checkbox"/> Y-G-2

Start Time :
End Time :

<input type="checkbox"/> R-Y-G	<input type="checkbox"/> R-Y-G
<input type="checkbox"/> R-Y-G-2	<input type="checkbox"/> R-Y-G-2
<input type="checkbox"/> R-G-2	<input type="checkbox"/> R-G-2
<input type="checkbox"/> Y-G-2	<input type="checkbox"/> Y-G-2

Start Time :
End Time :

<input type="checkbox"/> R-Y-G	<input type="checkbox"/> R-Y-G
<input type="checkbox"/> R-Y-G-2	<input type="checkbox"/> R-Y-G-2
<input type="checkbox"/> R-G-2	<input type="checkbox"/> R-G-2
<input type="checkbox"/> Y-G-2	<input type="checkbox"/> Y-G-2

Start Time :
End Time :

<input type="checkbox"/> R-Y-G	<input type="checkbox"/> R-Y-G
<input type="checkbox"/> R-Y-G-2	<input type="checkbox"/> R-Y-G-2
<input type="checkbox"/> R-G-2	<input type="checkbox"/> R-G-2
<input type="checkbox"/> Y-G-2	<input type="checkbox"/> Y-G-2

Fig. 4. A study paper prepared and used to test the performance of the examined red light violation detection system.

The data to be used within the scope of the study were collected by the researchers from the Akdeniz University with the help of field observations and video camera recordings made in October 2016. The video cameras which are positioned before the arms of the intersection were used to record the vehicle passing and the state of the traffic lights. For each intersection leg, a control vehicle was used with the coordination of the observers to provide safe and reliable investigation (See Figure 5). One of the researcher also registered if the provided scenario was successfully detected by the system or failed. The all investigation phase was completed in 20 minutes for each intersection by the researchers composed of three members. Not only the control vehicle but also the violations of the other vehicles were also recorded and considered in the study.

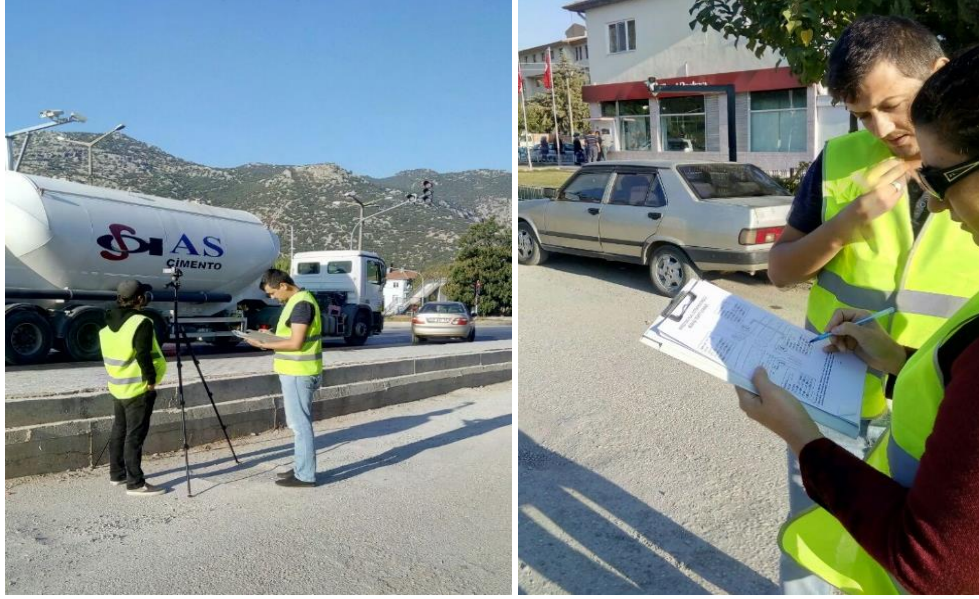


Fig.5. On-site control of the system.

4. Investigation of the System and Findings

The violations were transferred to a software under the control of the operator. In the Figure 6, the violations of the control vehicle and other drivers during the system testing period are shown in the control software.

Plaka	Tarih	Plaka Noktası	İhlal/Karaliste	Tahsis	Araç Tır. P. Marka P. Model	P.İ.P.	Ticari Adı	Ma Geçiş Notu
07BDN75	25.10.2016 07:06:43	BELEDİYE KIRMIZI	KIRMIZI İŞİK İHLALI	<input type="checkbox"/>		There was no endpoint listening at	0	<input type="checkbox"/>
07BDN75	25.10.2016 07:14:24	BELEDİYE KIRMIZI	KIRMIZI İŞİK İHLALI	<input type="checkbox"/>		There was no endpoint listening at	0	<input type="checkbox"/>
07BDN75	25.10.2016 07:16:54	ANTALYA BURDUR KIRMIZI	KIRMIZI İŞİK İHLALI	<input type="checkbox"/>		There was no endpoint listening at	0	<input type="checkbox"/>
07BDN75	25.10.2016 07:20:52	BURDUR ANTALYA KIRMIZI	KIRMIZI İŞİK İHLALI	<input type="checkbox"/>		There was no endpoint listening at	0	<input type="checkbox"/>
07BDN75	25.10.2016 07:21:35	ANTALYA BURDUR KIRMIZI	KIRMIZI İŞİK İHLALI	<input type="checkbox"/>		There was no endpoint listening at	0	<input type="checkbox"/>
07BDN75	25.10.2016 07:29:24	BURDUR ANTALYA KIRMIZI	KIRMIZI İŞİK İHLALI	<input type="checkbox"/>		There was no endpoint listening at	0	<input type="checkbox"/>
07BDN75	25.10.2016 07:30:44	BURDUR ANTALYA KIRMIZI	KIRMIZI İŞİK İHLALI	<input type="checkbox"/>		There was no endpoint listening at	0	<input type="checkbox"/>
07SP682	25.10.2016 07:31:47	ZİRAAT KIRMIZI	KIRMIZI İŞİK İHLALI	<input type="checkbox"/>		There was no endpoint listening at	0	<input type="checkbox"/>
07BDN75	25.10.2016 07:42:19	BURDUR ANTALYA KIRMIZI	KIRMIZI İŞİK İHLALI	<input type="checkbox"/>		There was no endpoint listening at	0	<input type="checkbox"/>
07BDN75	25.10.2016 07:46:13	BURDUR ANTALYA KIRMIZI	KIRMIZI İŞİK İHLALI	<input type="checkbox"/>		There was no endpoint listening at	0	<input type="checkbox"/>
07BDN75	25.10.2016 07:59:04	ANTALYA BURDUR KIRMIZI	KIRMIZI İŞİK İHLALI	<input type="checkbox"/>		There was no endpoint listening at	0	<input type="checkbox"/>
07BDN75	25.10.2016 08:02:20	ZİRAAT KIRMIZI	KIRMIZI İŞİK İHLALI	<input type="checkbox"/>		There was no endpoint listening at	0	<input type="checkbox"/>
07BDN75	25.10.2016 08:02:47	BELEDİYE KIRMIZI	KIRMIZI İŞİK İHLALI	<input type="checkbox"/>		There was no endpoint listening at	0	<input type="checkbox"/>
07BDN75	25.10.2016 08:04:04	ZİRAAT KIRMIZI	KIRMIZI İŞİK İHLALI	<input type="checkbox"/>		There was no endpoint listening at	0	<input type="checkbox"/>
07BDN75	25.10.2016 08:10:18	ZİRAAT KIRMIZI	KIRMIZI İŞİK İHLALI	<input type="checkbox"/>		There was no endpoint listening at	0	<input type="checkbox"/>
	25.10.2016 08:10:47	BELEDİYE KIRMIZI	KIRMIZI İŞİK İHLALI	<input type="checkbox"/>		There was no endpoint listening at	0	<input type="checkbox"/>
	25.10.2016 08:15:59	BURDUR ANTALYA KIRMIZI	KIRMIZI İŞİK İHLALI	<input type="checkbox"/>		There was no endpoint listening at	0	<input type="checkbox"/>
	25.10.2016 08:21:09	BELEDİYE KIRMIZI	KIRMIZI İŞİK İHLALI	<input type="checkbox"/>		There was no endpoint listening at	0	<input type="checkbox"/>
	25.10.2016 08:21:10	BELEDİYE KIRMIZI	KIRMIZI İŞİK İHLALI	<input type="checkbox"/>		There was no endpoint listening at	0	<input type="checkbox"/>
	25.10.2016 08:23:54	BELEDİYE KIRMIZI	KIRMIZI İŞİK İHLALI	<input type="checkbox"/>		There was no endpoint listening at	0	<input type="checkbox"/>
	25.10.2016 08:35:17	BELEDİYE KIRMIZI	KIRMIZI İŞİK İHLALI	<input type="checkbox"/>		There was no endpoint listening at	0	<input type="checkbox"/>
	25.10.2016 08:35:24	BELEDİYE KIRMIZI	KIRMIZI İŞİK İHLALI	<input type="checkbox"/>		There was no endpoint listening at	0	<input type="checkbox"/>
	25.10.2016 08:40:15	BELEDİYE KIRMIZI	KIRMIZI İŞİK İHLALI	<input type="checkbox"/>		There was no endpoint listening at	0	<input type="checkbox"/>
	25.10.2016 08:44:10	BELEDİYE KIRMIZI	KIRMIZI İŞİK İHLALI	<input type="checkbox"/>		There was no endpoint listening at	0	<input type="checkbox"/>
	25.10.2016 08:49:39	BURDUR ANTALYA KIRMIZI	KIRMIZI İŞİK İHLALI	<input type="checkbox"/>		There was no endpoint listening at	0	<input type="checkbox"/>
	25.10.2016 09:08:48	BELEDİYE KIRMIZI	KIRMIZI İŞİK İHLALI	<input type="checkbox"/>		There was no endpoint listening at	0	<input type="checkbox"/>

Fig.6. A view from the software with the listed red light violations.

After the review of the software, the video recordings and field investigations were compared with the system output to check if the system works appropriate as shown in Figure 7.



Fig.7. The comparison of the red light violation detected (a) Red light violation detection system (b) researchers.

From the comparison of system and observation data, it was concluded that all the cameras of the red light violation detection system were properly working and all the violations were successfully detected by the applied system.

5. Results and Conclusions

It has been determined that devices belonging to the red light violation detection system, which are examined within the scope of the field observations, are actively working. From field observations and analyzes, it was concluded that eight different scenarios proposed to study the performance of each leg of a 4-leg signalized intersection were sufficient and efficient to examine the performance of red light violation detection systems. It has been determined that the violations determined by the system software and field tests give exactly the same results. In particular, none of the critical passing which would not be regarded as violations were not counted by the system. This shows that the system detects the violations in a reliable way. The system also correctly captured all of the passages not only during the transition between green to red but also red to green state of the traffic lights. It is important to note that this proposed investigation technique tries to consider the interests of the drivers and minimize or prevent unfairly traffic tickets. It was assumed that integrated detection systems for the signalized intersections considering the phase times will be developed and loop detectors will also be included to the detection systems in the future. For this reason, it is expected that our test methodology will be more prominent and developed by the implementation of these new generation systems.

Acknowledgments

The authors would like to thank Bilge Elektronik Güvenlik Bilgisayar Sistemleri ve İnşaat San. Tic. Ltd. Şti for their kindly help and support for the study.

References

- [1] Ghasemlou, K., Aydin, M., Yildirim, M., Prediction of pedal cyclists and pedestrian fatalities from total monthly accidents and registered private car numbers. *Archives of Transport*, 34(2), 29--35, 2015
- [2] Coruh, E., Bilgic, A., Tortum, A., Accident analysis with aggregated data: The random parameters negative binomial panel count data model. *Analytic methods in accident research*, 7, 37-49, 2015.
- [3] KGM, Trafik Kazaları Özeti 2011. 2011, Trafik Güvenliği Dairesi Başkanlığı: Ankara.
- [4] KGM, Trafik Kazaları Özeti 2012. 2012, Trafik Güvenliği Dairesi Başkanlığı: Ankara.
- [5] KGM, Trafik Kazaları Özeti 2013. 2013, Trafik Güvenliği Dairesi Başkanlığı: Ankara.
- [6] KGM, Trafik Kazaları Özeti 2014. 2014, Trafik Güvenliği Dairesi Başkanlığı: Ankara.
- [7] KGM, Trafik Kazaları Özeti 2015. 2015, Trafik Güvenliği Dairesi Başkanlığı: Ankara.
- [8] Yung, N.H.C., Lai, A.H., An effective video analysis method for detecting red light runners. *IEEE Transactions on Vehicular Technology*, 50(4), 1074-1084, 2001.
- [9] Fitzsimmons, E.J., The effectiveness of Iowa's automated red light running enforcement programs 2007; ProQuest, 2007.
- [10] Günay, B., Erdemir, G., Lateral Analysis of Longitudinal Headways in Traffic Flow. *International Journal of Engineering and Applied Sciences*, 3, 90-100, 2011.
- [11] Saha, S., Basu, S., Nasipuri, M., Basu, D.K., Development of an automated red light violation detection system (RLVDS) for Indian vehicles. *arXiv preprint arXiv:1003.6052*, 2010.
- [12] Passetti, K., Hicks, T., Use of automated enforcement for red light violations. 1997, the University.
- [13] Singh, H., Singh, S.J., Singh, R.P., Red Light Violation Detection Using RFID. *Proceedings of 'I-Society*, 2012.
- [14] Heidari, M., Monadjemi, S.A., Effective Video Analysis for Red Light Violation Detection. *Journal of Basic and Applied Scientific Research*, 3(1s), 642-646, 2013.
- [15] Brasil, R.H., Machado, A.M.C., Automatic Detection of Red Light Running Using Vehicular Cameras. *IEEE Latin America Transactions*, 15(1), 81-86, 2017.
- [16] Baguley, C., 'Running the red' at signals on high-speed roads. *Traffic engineering and control*, 29(7-8), 415-420, 1988.
- [17] Yang, C., Najm, W.G., Analysis of red light violation data collected from intersections equipped with red light photo enforcement cameras. 2006.
- [18] Lum, K., Wong, Y., Impacts of red light camera on violation characteristics. *Journal of transportation engineering*, 129(6), 648-656, 2003.
- [19] Schattler, K., Hill, C., Datta, T. Clearance interval design and red light violations. *Today's Transportation Challenge: Meeting Our Customer's Expectations*, Year.
- [20] Ruby, D.E., Hobeika, A.G., Assessment of red light running cameras in Fairfax County, Virginia. *Transportation Quarterly*, 57(3), 33-48, 2003.
- [21] Chin, H.C., Haque, M., Effectiveness of red light cameras on the right-angle crash involvement of motorcycles. *Journal of advanced transportation*, 46(1), 54-66, 2012.

- [22] Shin, K., Washington, S., The impact of red light cameras on safety in Arizona. *Accident Analysis & Prevention*, 39(6), 1212-1221, 2007.
- [23] Malone, B., Suggett, J., Stewart, D. Evaluation of the red light camera enforcement pilot project. ITE 2005 Annual Meeting and Exhibit Compendium of Technical Papers, Year.
- [24] Burkey, M.L., Obeng, K., A detailed investigation of crash risk reduction resulting from red light cameras in small urban areas. 2004.

Optimisation of Refrigeration System with Two-Stage and Intercooler Using Fuzzy Logic and Genetic Algorithm

Bayram Kılıç

Mehmet Akif Ersoy University, Bucak Emin Gülmez Vocational School, Burdur
E-mail address: bayramkilic@mehmetakif.edu.tr

Received date: February 2017

Abstract

Two-stage compression operation prevents excessive compressor outlet pressure and temperature and this operation provides more efficient working condition in low-temperature refrigeration applications. Vapor compression refrigeration system with two-stage and intercooler is very good solution for low-temperature refrigeration applications. In this study, refrigeration system with two-stage and intercooler were optimized using fuzzy logic and genetic algorithm. The necessary thermodynamic characteristics for optimization were estimated with Fuzzy Logic and liquid phase enthalpy, vapour phase enthalpy, liquid phase entropy, vapour phase entropy values were compared with actual values. As a result, optimum working condition of system was estimated by the Genetic Algorithm as -6.0449 °C for evaporator temperature, 25.0115 °C for condenser temperature and 5.9666 for COP. Moreover, irreversibility values of the refrigeration system are calculated.

Keywords: Optimisation, Refrigeration System, COP, Genetic Algorithm, Fuzzy Logic

1. Introduction

Mohanraja et al. have been reviewed energy and exergy analysis of refrigeration, air conditioning and heat pump systems using artificial neural networks. Their study shown that ANN method has given satisfactory results for air conditioning and heat pump systems [1]. Zhao et al. have used a model-based optimization method for vapour compression refrigeration cycle. They have used modified genetic algorithm as optimization method. Modified genetic algorithm results have compared with traditional methods. As a result of study, they have shown that data obtained from their study is suitable for actual systems [2]. Sanaye and Asgari were investigated performance of the thermal modelling of gas engine driven air-to-water heat pump system with engine heat recovery heat exchangers for the heating mode of operation. In their study, artificial neural network and the multi-objective genetic algorithm optimization method were used to prediction of thermodynamic characteristics of system components. Results of study were compared with experimental data. Their results showed that acceptable for operating pressure, gas engine fuel consumption, outlet water temperature, engine rotational speed, and system primary energy ratio [3]. Kamar et al. have made to estimation cooling capacity, compressor power input and the coefficient of performance of the automotive air-conditioning system for passenger car using artificial neural networks model. They have constructed experimental system for this study. The experimental system was operated at steady-state conditions. And they have changed the compressor speed, air temperature at evaporator



inlet, air temperature at condenser inlet and air velocity at evaporator inlet. Root mean square error (RMSE) was obtained in the range of %0.33-0.95 and mean square error (MSE) were obtained between 1.09×10^5 and 9.05×10^5 in their study [4]. Esen and Inalli have been examined to estimation of performance of a vertical ground source heat pump system with artificial neural network and an adaptive neuro-fuzzy inference system. Esen and Inalli have compared that obtained data from artificial neural network and an adaptive neuro-fuzzy inference system. Their results showed that adaptive neuro-fuzzy inference system (ANFIS) method has given more consistent results for estimation of performance of vertical ground source heat pump system [5]. Şencan et al. have used artificial neural network method for determination of thermophysical properties of refrigerants. These properties are heat conduction coefficient, dynamic viscosity, kinematic viscosity, thermal diffusivity, density, specific heat capacity of refrigerants. They worked on five refrigerants. Five refrigerants are: R413A, R417A, R422A, R422D and R423A. As a result of their study, they have derived an equation for estimation of thermodynamic properties of the refrigerants [6].

In the literature, experimental studies on optimization of refrigeration system with two-stage and intercooler are very limited. In this study, refrigeration system with two-stage and intercooler were optimized using fuzzy logic and genetic algorithm.

2. Modelling, Solkane Program, Fuzzy Logic and Genetic Algorithm

2.1. Solkane Program

The necessary thermodynamic properties for optimization were calculated by Solkane program. Solkane program is a powerful calculation program for thermodynamic properties. It calculates the thermodynamic substance data and transport properties of all refrigerants and some CFCs. It contains modules for the calculation of a total of 7 different ones and two-step cycle processes and for dimensioning of a refrigerant's pipe lines. Besides, Solkane program contains 5 different cooling cycle and 2 different Rankine cycle in the program structure [10].

2.2. Fuzzy Logic

Fuzzy Logic can be described as expression of uncertainty and solid mathematical a scheme that established to work with uncertainty. As is known in statistics and probability theory, works with certainty not with uncertainty. But, environment in which people live is filled with more uncertainty. So, should work with uncertainty for in order to understand mankind's the ability to draw conclusions.

In the logic of Aristotle are black or white. In the real world, you cannot find the full black or full white. Fuzzy logic almost exclusively works with grey in accordance with the real life. There are black or white in extreme cases. Complex systems are difficult controlled and modeling with classical logic methods. Fuzzy logic that people are relieved of the obligation and provide the ability to define a more qualitative.

Fuzzy Logic is used for applications such as cameras, washing machines, air conditioning and automatic transmission lines. Furthermore, it is used in space exploration and aerospace industries. A fuzzy logic model consists of four components. These components are fuzzifiers, the inference engine, the defuzzifier and a fuzzy rule base (Figure 1).

In the fuzzy logic, “and method”, “or method”, “implication”, “aggregation” ve “defuzzification” are used as “min”, “max”, “min”, “max”, “centroid”. The Mamdani method was applied. The fitness function of all variables in fuzzy logic is chosen as "trimf".

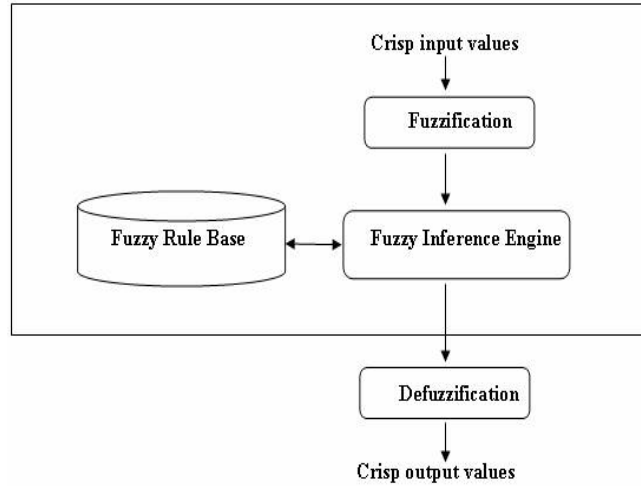


Fig.1. Basic flow chart of fuzzy logic [9]

Input values in the fuzzifier are fuzzified into linguistic values to be associated to the input linguistic variables. After fuzzification, the inference engine refers to the fuzzy rule base containing fuzzy IF-THEN rules to derive the linguistic values for the intermediate and output linguistic variables. The defuzzifier produces the final values from the output values and these output values are available.

2.3. Genetic Algorithm

The genetic algorithm is a method for solving both constrained and unconstrained optimization problems that is based on natural selection, the process that drives biological evolution. The genetic algorithm repeatedly modifies a population of individual solutions. At each step, the genetic algorithm selects individuals at random from the current population to be parents and uses them to produce the children for the next generation. Over successive generations, the population “evolves” toward an optimal solution [9-]. Basic flow chart of Genetic Algorithm was given in Figure 2.

Genetic algorithm procedure is as follows;

Step 1. Start: Initial population is created after N chromosomes with m pieces individuals are produced as randomly for to solve of the problem. Or, the initial population may also be created from specific individuals.

Step 2. Fitness: Objective function is calculated for each individual in the population.

Step 3. New population: Following steps are repeated until the formation of a new population;

a) Selection: According to the fitness value of the objective function selected individuals from the population are thrown into the match’s pool for crossover.

b) Crossover: Individuals that selected from matching pool are crossed among themselves until crossover rate child individual.

c) Mutation: Any chromosomes of selected individual or individuals from in the population are reset and instead a new value is assigned.

d) Admission: The first population, children and mutated individuals constitute a new population.

Step 4. Replacement: Consisting new population are sorted according to fitness value and until the number of individuals in the population is assigned as the new initial population.

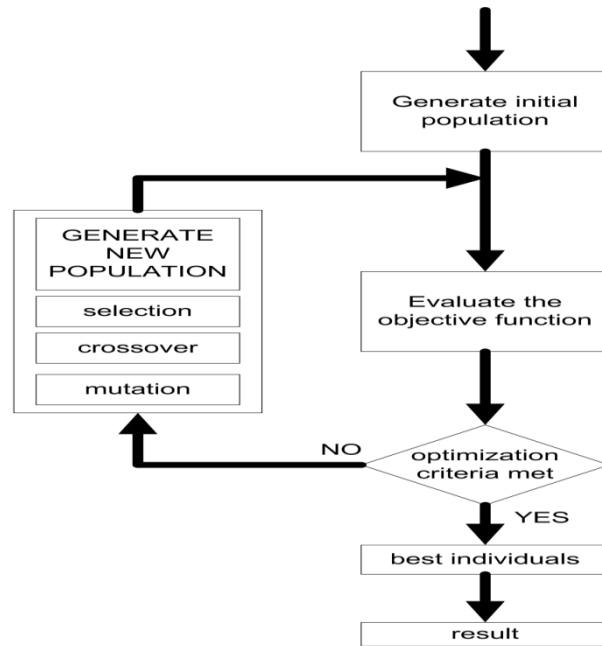


Fig.2. Basic flow chart of Genetic Algorithm [7]

Step 5. Test: If the program finishing requirement is happening, the program is stopped.

Step 6. Cycle: Otherwise, the program go back to step 2.

3. Results and discussion

In this study, refrigeration system with two-stage and intercooler were optimized by using fuzzy logic and genetic algorithm. The required thermodynamic characteristics for optimization were estimated with Fuzzy Logic and these values were compared with actual values.

Input- output parameter used in fuzzy logic was given in Figure 3. MATLAB Fuzzy Logic Toolbox is used for estimation for thermodynamic properties in the study. Mamdani type fuzzy inference system (FIS) was used. Type of membership function is trimf. 40 piece training values and 15 piece test values have been used in fuzzy logic. 4 input values and 14 output values in system have taken into consideration in fuzzy logic. Input values are evaporator temperature, evaporator pressure, condenser temperature and condenser pressure. Evaporator temperature is in the range of -6°C to -24

°C, the condenser temperature is in the range from 25 °C to 40 °C. Output values are enthalpy values, entropy values, the mass flow rate, electric charge of the high and low pressure compressors for all in each point of the system. Some of the rules used in fuzzy logic technic are given in Figure 4.

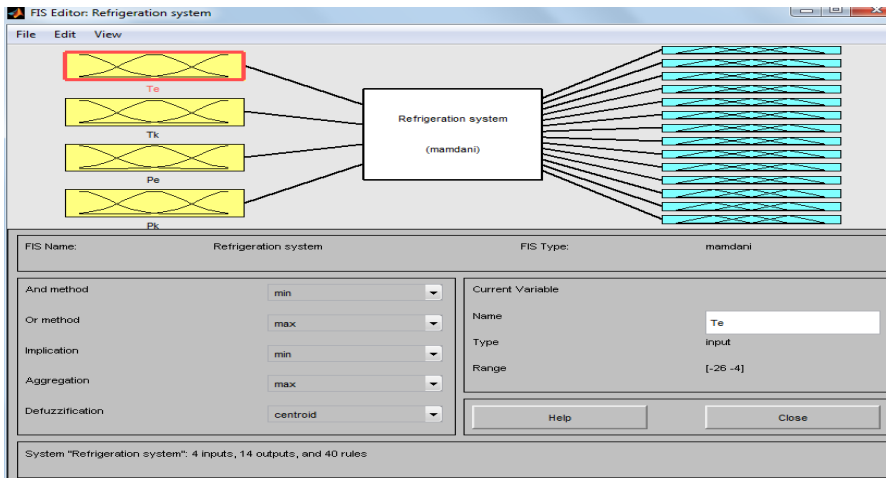


Fig.3. Input-output values for refrigeration system in fuzzy logic

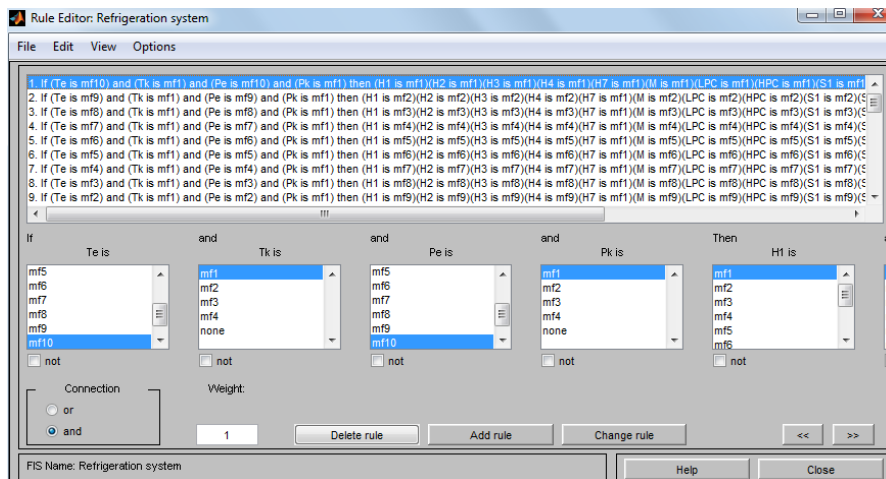


Fig.4. Rules of fuzzy logic

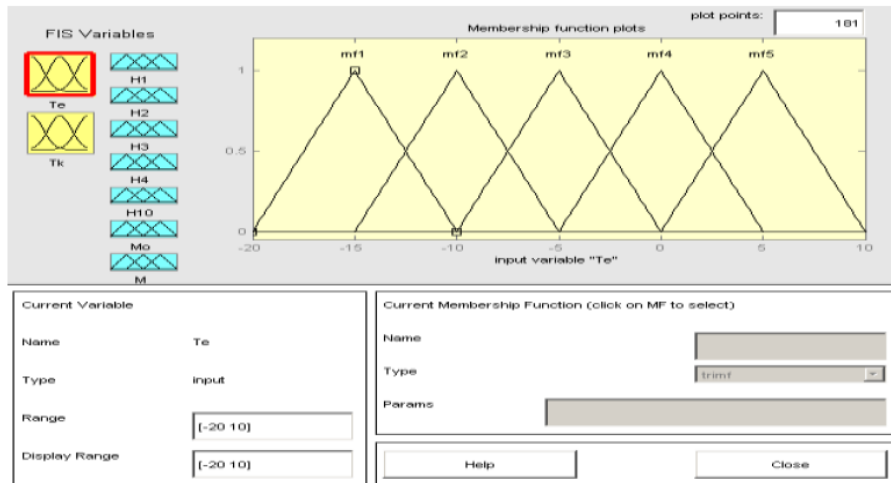


Fig.5. Membership Function (for evaporator temperature)

Comparison of actual high pressure compressor outlet enthalpy values and estimated enthalpy values was given in Figure 6 as exemplarily. Comparison of actual high pressure compressor outlet entropy values and estimated entropy values was given in Figure 7 as exemplarily.

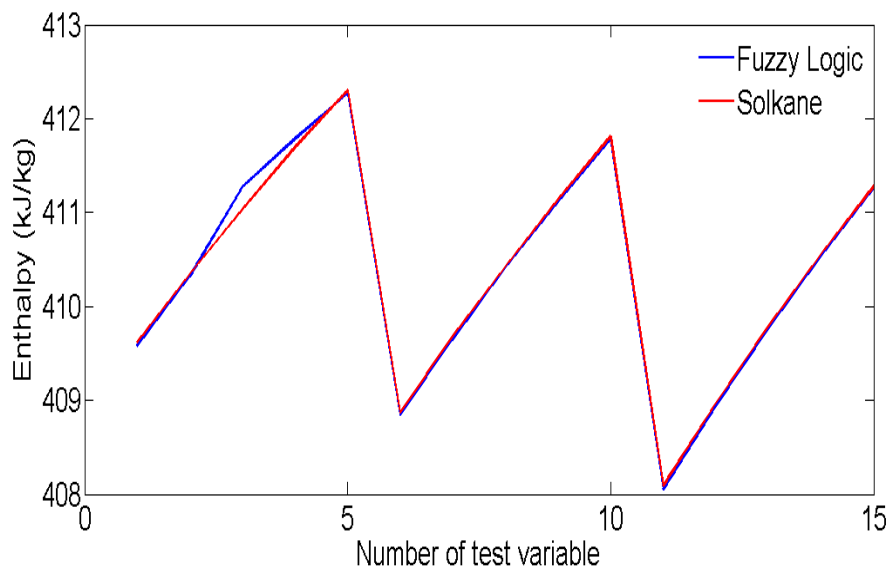


Fig.6. Comparison of actual high pressure compressor outlet enthalpy values and estimated enthalpy values

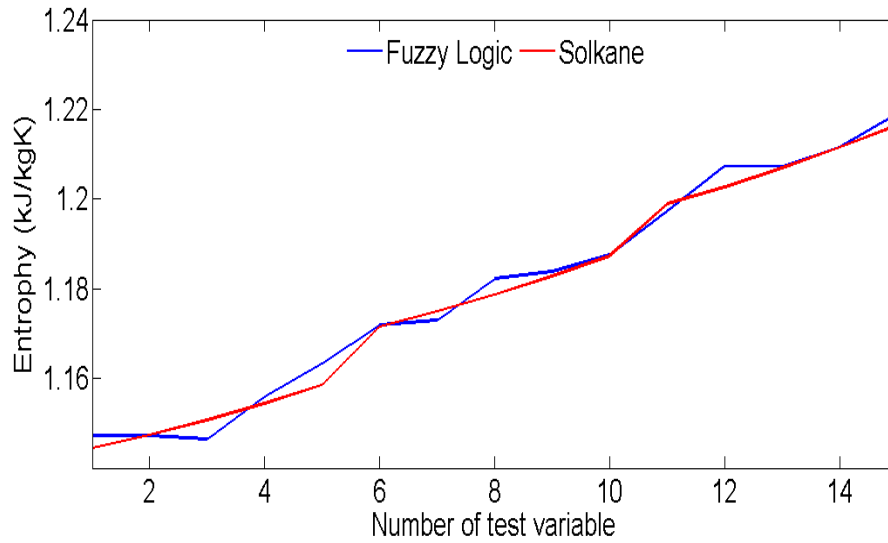


Fig.7. Comparison of actual high pressure compressor outlet entropy values and estimated entropy values

In Table 1, average absolute relative error values related to the thermodynamic values are given. As can be seen from Table 1, fuzzy logic technic has provided a good estimate values.

Table 1. Average absolute relative error values.

	Average Absolute Relative Error
Evaporator output enthalpy	0
Low Pressure Compressor output enthalpy	1.13×10^{-4}
High Pressure Compressor input enthalpy	8.27×10^{-4}
Condenser input enthalpy	4.07×10^{-5}
Evaporator input enthalpy	2.2×10^{-3}
Mass flow rate	1.78×10^{-5}
Evaporator output entropy	6×10^{-9}
Low Pressure Compressor output entropy	1.75
High Pressure Compressor input entropy	1.77
Condenser input entropy	1.75
Condenser output entropy	1.76
Evaporator input entropy	1.15
Electric charge of the Low Pressure Compressor	1.5×10^{-5}
Electric charge of the High Pressure Compressor	1.15×10^{-5}

Table 2. Comparison between actual enthalpy values and enthalpy values estimated from Fuzzy Logic for R-134a

Temperature	Pressure	Liquid Phase Enthalpy			Vapour Phase Enthalpy		
T (°C)	P (bar)	Actual Values (kJ/kg)	Estimated values with Fuzzy Logic (kJ/kgK)	Error	Actual Values (kJ/kg)	Estimated values with Fuzzy Logic (kJ/kgK)	Error
-24	1.11	168.41	168.42	0.01	384.04	384.04	0
-23	1.16	169.69	169.7	0.01	384.66	384.65	0.01
-22	1.22	170.98	170.98	0	385.28	385.28	0
-21	1.27	172.27	172.28	0.01	385.89	385.89	0
-20	1.33	173.56	173.55	0.01	386.51	386.51	0
-19	1.39	174.85	174.86	0.01	387.12	387.12	0
-18	1.45	176.15	176.16	0.01	387.73	387.73	0
-17	1.51	177.45	177.45	0	388.34	388.35	0.01
-16	1.57	178.75	178.76	0.01	388.95	388.95	0
-15	1.64	180.06	180.07	0.01	389.56	389.56	0
-14	1.71	181.36	181.36	0	390.17	390.17	0
-13	1.78	182.68	182.68	0	390.77	390.77	0
-12	1.85	183.99	183.99	0	391.38	391.38	0
-11	1.93	185.31	185.31	0	391.98	391.98	0
-10	2.01	186.63	186.62	0.01	392.58	392.58	0
-9	2.09	187.95	187.96	0.01	393.18	393.18	0
-8	2.17	189.28	189.28	0	393.78	393.78	0
-7	2.25	190.61	190.61	0	394.37	394.37	0
-6	2.34	191.94	191.94	0	394.97	394.97	0
-5	2.43	193.27	193.28	0.01	395.56	395.55	0.01
-4	2.53	194.61	194.61	0	396.15	396.15	0
-3	2.62	195.95	195.96	0.01	396.74	396.74	0
-2	2.72	197.3	197.3	0	397.32	397.32	0
-1	2.82	198.64	198.66	0.02	397.91	397.9	0.01
0	2.93	200	200	0	398.49	398.49	0

Table 3. Comparison between actual entropy values and entropy values estimated from Fuzzy Logic for R-134a.

Temperature	Pressure	Liquid Phase Entropy			Vapour Phase Entropy		
T (°C)	P (bar)	Actual Values (kJ/kgK)	Estimated values with Fuzzy Logic (kJ/kgK)	Error	Actual Values (kJ/kgK)	Estimated values with Fuzzy Logic (kJ/kgK)	Error
-24	1.11	0.8793	0.87931	1.10 ⁻⁵	1.745	1.745	0
-23	1.16	0.8845	0.88443	7.10 ⁻⁵	1.744	1.744	0
-22	1.22	0.8896	0.88965	5.10 ⁻⁵	1.7431	1.7431	0
-21	1.27	0.8948	0.89473	7.10 ⁻⁵	1.7421	1.7421	0
-20	1.33	0.8999	0.89987	3.10 ⁻⁵	1.7412	1.7411	1.10 ⁻⁴
-19	1.39	0.905	0.90502	2.10 ⁻⁵	1.7403	1.7403	0
-18	1.45	0.9101	0.91007	3.10 ⁻⁵	1.7394	1.7394	0
-17	1.51	0.9152	0.91516	4.10 ⁻⁵	1.7385	1.7386	1.10 ⁻⁴
-16	1.57	0.9203	0.92034	4.10 ⁻⁵	1.7377	1.7378	1.10 ⁻⁴
-15	1.64	0.9254	0.92535	5.10 ⁻⁵	1.7369	1.7369	0
-14	1.71	0.9304	0.93044	4.10 ⁻⁵	1.7361	1.7361	0
-13	1.78	0.9355	0.93543	7.10 ⁻⁵	1.7353	1.7354	1.10 ⁻⁴
-12	1.85	0.9405	0.94049	1.10 ⁻⁵	1.7346	1.7346	0
-11	1.93	0.9455	0.94548	2.10 ⁻⁵	1.7338	1.7338	0
-10	2.01	0.9505	0.95046	4.10 ⁻⁵	1.7331	1.7331	0
-9	2.09	0.9555	0.95547	3.10 ⁻⁵	1.7324	1.7324	0
-8	2.17	0.9605	0.96045	5.10 ⁻⁵	1.7317	1.7316	1.10 ⁻⁴
-7	2.25	0.9655	0.96546	4.10 ⁻⁵	1.731	1.731	0
-6	2.34	0.9705	0.97052	2.10 ⁻⁵	1.7304	1.7304	0
-5	2.43	0.9754	0.97542	2.10 ⁻⁵	1.7297	1.7299	2.10 ⁻⁴
-4	2.53	0.9804	0.98043	3.10 ⁻⁵	1.7291	1.7291	0
-3	2.62	0.9853	0.98533	3.10 ⁻⁵	1.7285	1.7285	0
-2	2.72	0.9902	0.99022	2.10 ⁻⁵	1.7279	1.7279	0
-1	2.82	0.9951	0.99512	2.10 ⁻⁵	1.7273	1.7272	1.10 ⁻⁴
0	2.93	1	1	0	1.7267	1.7266	1.10 ⁻⁴

Optimum working conditions of refrigeration system with two-stage and intercooler were determined in order to obtain maximum cooling coefficient of performance (COP) by the Genetic Algorithm. The objective functions used in Genetic Algorithm are:

$$COP_{max.} = \frac{\text{Cooling load}}{\text{Power input}} \quad (1)$$

Figure 8 shows results of genetic algorithm for the condenser temperature with COP value. Evaporator temperature is constant. Figure 9 shows results of genetic algorithm for the evaporator temperature with COP value. Condenser temperature is constant.

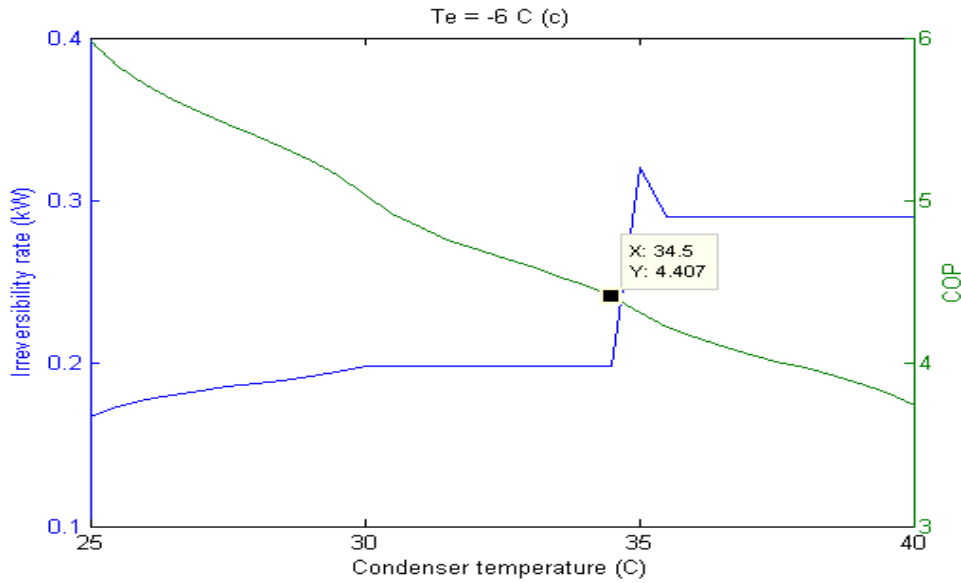


Fig.8. Genetic algorithm results for irreversibility and COP values depend on condenser temperature variation.

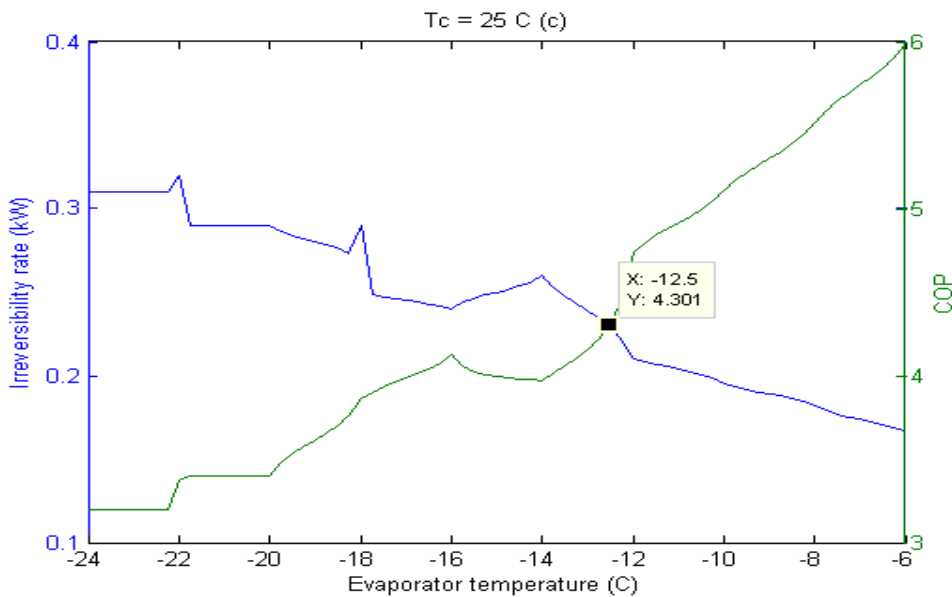


Fig.9. Genetic algorithm results for irreversibility and COP values depend on evaporator temperature variation.

Genetic algorithm results for COP values depend on condenser and evaporator temperatures are shown in Figure 10. In this study, optimum working condition of system was estimated by the Genetic Algorithm as $-6.0449\text{ }^{\circ}\text{C}$ for evaporator temperature, $25.0115\text{ }^{\circ}\text{C}$ for condenser temperature and 5.9666 for COP.

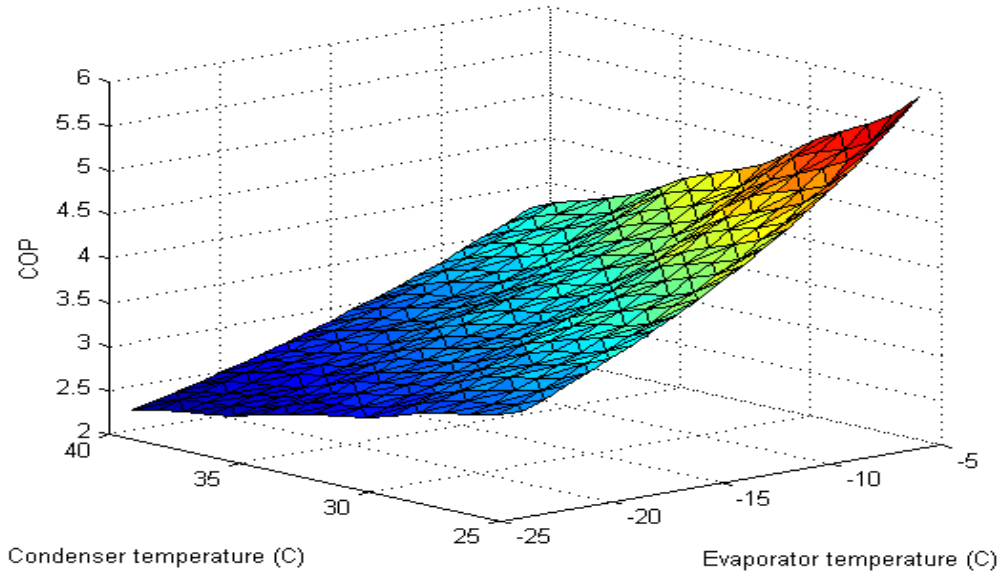


Fig.10. Genetic algorithm results for COP values.

Genetic algorithm results for irreversibility values depend on condenser and evaporator temperatures are shown in Figure 11. In this study, irreversibility rate was 0.45 kW as the highest value. In the Pareto analysis, optimum values of refrigeration system were forecasted by the Genetic Algorithm as 5.98 for COP, 0.167 kW for irreversibility rate.

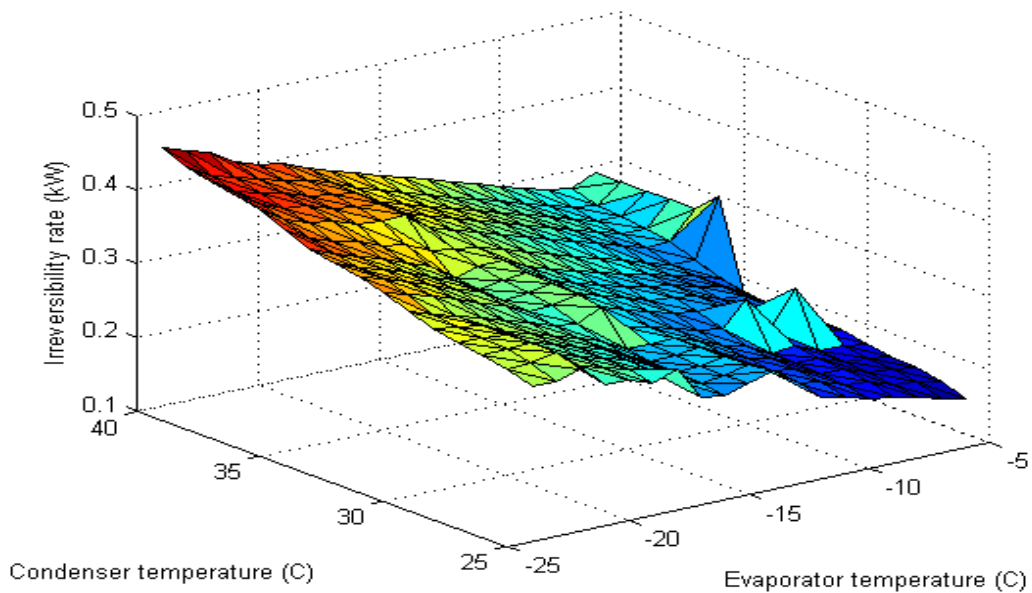


Fig.11. Genetic algorithm results for irreversibility values.

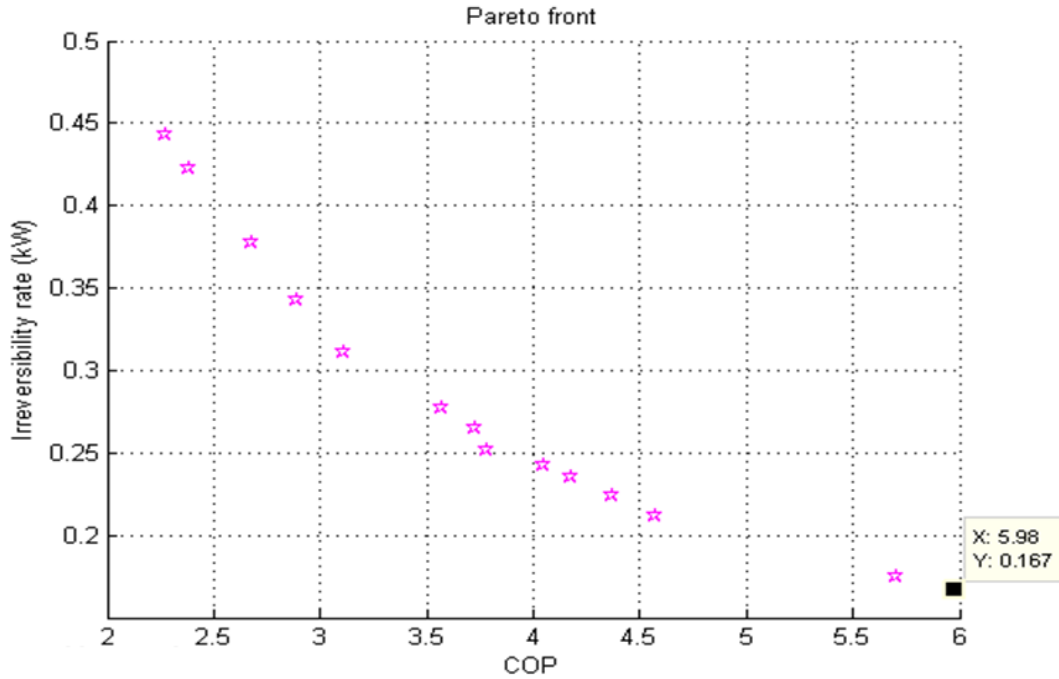


Fig.12. Pareto analysis of the refrigeration system.

4. Conclusions

In this study, refrigeration system with two-stage and intercooler were optimized using fuzzy logic and genetic algorithm. The necessary thermodynamic characteristics for optimization were forecasted with Fuzzy Logic and these values were compared with actual results. As results of this study, optimum working condition of refrigeration system was estimated by the Genetic Algorithm as -6.0449 °C for evaporator temperature, 25.0115 °C for condenser temperature and 5.9666 for COP. Moreover, irreversibility values of the refrigeration system were calculated and irreversibility rate was 0.45 kW as the highest value. This work shows that Genetic Algorithm can use for determining optimum working conditions of the refrigeration system with two-stage and intercooler.

From the literature review aforesaid above, it is seen that basic computational intelligence techniques are used in the transcritical CO₂ one-stage vapor compression cycles. However, an ANN method has not been carried out for the coefficient of performance (COP) in the transcritical CO₂ one-stage vapor compression cycles yet. This paper is focused on the applicability of ANN methods for estimation the coefficient of performance (COP).

References

- [1] Mohanraja, M., Jayaraj, S., Muraleedharan, C., Applications of artificial neural networks for refrigeration. Air-conditioning and heat pump systems—A review. *Renewable and Sustainable Energy Reviews*, 16, 1340-1358, 2012.

- [2] Zhao, L., Cai, W., Ding, X., Chang L., Model-based optimization for vapor compression refrigeration cycle. *Energy*, 55, 392-402, 2013.
- [3] Sanaye, S., Asgari, H., Thermal modeling of gas engine driven air to water heat pump systems in heating mode using genetic algorithm and Artificial Neural Network methods. *International Journal of Refrigeration*, 36, 2262-2277, 2012.
- [4] Kamar, H., Ahmad, R., Kamsah, N., Mustafa, A., Artificial neural networks for automotive air-conditioning systems performance prediction. *Applied Thermal Engineering*, 50, 63-70, 2013.
- [5] Esen, H., Inalli, M., ANN and ANFIS models for performance evaluation of a vertical ground source heat pump system. *Expert Systems with Applications*, 37, 8134-8147, 2010.
- [6] Sencan, A., Köse, I., Selbas, R., Prediction of thermophysical properties of mixed refrigerants using artificial neural network. *Heat Mass Transfer*, 47, 1553-1560, 2011.
- [7] Chakraborty, D., Sharma, C., Abhishek, B., Malakar, T., Distribution System Load Flow Solution Using Genetic Algorithm. *ICPS'09 International Conference on power systems*, 1–6, 2009.
- [8] Özdemir, A., Lim, Y., Singh, C., Post-outage reactive power flow calculations by genetic algorithms: constrained optimization approach. *IEEE Transactions on Power Systems*, 20, 1266-1272, 2005.
- [9] Sencan, A., Kılıç, B., Kılıç, U., Optimization of heat pump using fuzzy logic and genetic algorithm. *Heat Mass Transfer*, 47, 1553-1560, 2011.
- [10] Kılıç, B., Alternative Approach For Thermal Analysis Of Transcritical Co₂ One-Stage Vapor Compression Cycles. *International Journal of Engineering & Applied Sciences (IJEAS)*, 8, 1-6, 2016.

Frequency and Mode Shapes of Au Nanowires Using the Continuous Beam Models

Hayri Metin Numanoglu, Kadir Mercan, Ömer Civalek*

Akdeniz University, Civil Engineering Department,
Division of Mechanics, Antalya-TURKIYE
*E-mail address: civalek@yahoo.com

Received date: March 2017

Abstract

Free vibration analysis of Au nanowires has been investigated. Au nanowire is modeled as a thin beam by using the continuum theory. Three-different cross-sections such as circular, rectangular and triangular are taken into consideration for ultra thin nanowires. Frequency values have been obtained for different geometric parameters and simply supported boundary condition (S-S). This study is helpful for design of the nanowires based instruments in modern Nanoelectromechanical systems (NEMS).

Keywords: Nanowires, Au, Frequency, Mode shapes, Mechanical properties.

1. Introduction

It is known that the nanowire is one-dimensional nanostructure. Nanowires have many novel and potential applications due to their unique physical properties such as electrical, magnetic, optical, and mechanical. Many of previous theoretical investigations in this area employed molecular dynamic simulations to obtain the mechanical properties [1-7]. Frequency properties are important for some nanowire applications such as actuators, probes, resonators, and sensors. In this study, free vibration analysis of Au nanowire is investigated. Nanowire is modeled via Euler-Bernoulli beam as mechanical model. The effects of cross-section, mode numbers and dimension on frequency have been discussed.

2. Discrete singular convolution (DSC)

The method of discrete singular convolution (DSC) is a novel kind numerical approach for numerical solutions of differential equations [8]. Wei and his co-workers first applied the DSC algorithm to solve solid and fluid mechanics problem [9-18]. Civalek [19-30] gives numerical solution of free vibration problem of rotating and laminated conical shells and plates. Consider a distribution, T and $\eta(t)$ as an element of the space of the test function. A singular convolution can be defined by [9]



$$F(t) = (T * \eta)(t) = \int_{-\infty}^{\infty} T(t-x)\eta(x)dx \quad (1)$$

where $T(t-x)$ is a singular kernel. For example, singular kernels of delta type [10]

$$T(x) = \delta^{(n)}(x); \quad (n=0,1,2,\dots). \quad (2)$$

Kernel $T(x) = \delta(x)$ is important for interpolation of surfaces and curves, and $T(x) = \delta^{(n)}(x)$ for $n>1$ are essential for numerically solving differential equations. With a sufficiently smooth approximation, it is more effective to consider a discrete singular convolution [11]

$$F_{\alpha}(t) = \sum_k T_{\alpha}(t-x_k)f(x_k), \quad (3)$$

The Shannon's kernel is regularized as [11]

$$\delta_{\Delta,\sigma}(x-x_k) = \frac{\sin[(\pi/\Delta)(x-x_k)]}{(\pi/\Delta)(x-x_k)} \exp\left[-\frac{(x-x_k)^2}{2\sigma^2}\right]; \quad \sigma>0. \quad (4)$$

Equation (4) can also be used to provide discrete approximations to the singular convolution kernels of the delta type [12]

$$f^{(n)}(x) \approx \sum_{k=-M}^M \delta_{\Delta}(x-x_k)f(x_k), \quad (5)$$

3. Euler-Bernoulli beam model

Beam model is widely used for nano-scaled components analysis [31-33]. Governing equation of motion for a beam is given as [35]:

$$EI \frac{\partial^4 w(x,t)}{\partial x^4} + \rho A \frac{\partial^2 w(x,t)}{\partial t^2} = f(x,t) \quad (6)$$

By using the analytical (separation of variables) and the DSC methods, related equation is solved for three different cross-sections (Table 1) and S-S boundary condition listed in Table 2. The resulting frequency equation can be expressed as follows:

$$\omega = \frac{n^2 \pi^2}{L^2} \sqrt{\frac{EI}{\rho A}} \quad (7)$$

4. Numerical results

By using the three-different cross sections given in Table 1, frequency values are obtained for S-S nanowires for Au material. The Young modulus of Au used in calculations is 79 GPa, and mass density is $\rho = 19.3 \text{ gr/cm}^3$. Results are depicted in Table 2 and Figs 1-2, respectively. The results given in Table 2 are obtained via DSC method. The other results are obtained via analytical.

Table 1. Cross-sections, areas and moment of inertia formulas of nanowire

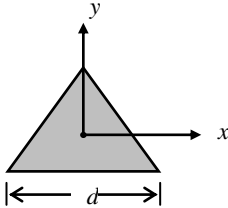
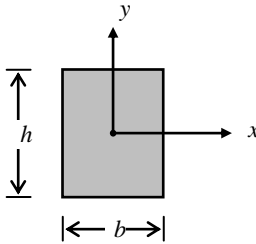
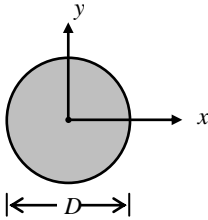
<i>Cross-section</i>	<i>Name</i>	<i>Area</i>	<i>Moment of Inertia</i>
	Triangular	$A = \frac{d\sqrt{3}}{4}$	$I_x = \frac{d^4\sqrt{3}}{96}$
	Rectangular	$A = bh$	$I_x = \frac{bh^3}{12}$
	Circular	$A = \frac{\pi D^2}{4}$	$I_x = \frac{\pi D^4}{64}$

Table 2. Frequency values (GHz) for three-different cross sections

<i>Mode Numbers</i>	$A = 10 \text{ nm}^2, L = 50 \text{ nm}$		
	<i>Circular</i> $D = 3.57 \text{ nm}$	<i>Rectangular</i> $h = 5 \text{ nm}$ $b = 2 \text{ nm}$	<i>Triangular</i> $d = 4.81 \text{ nm}$
1	7.1346	11.5345	7.8439
2	28.5285	46.1207	31.6972
3	64.1647	103.7664	70.5801
4	114.0682	184.4720	125.4836
5	178.2203	288.2246	196.0677

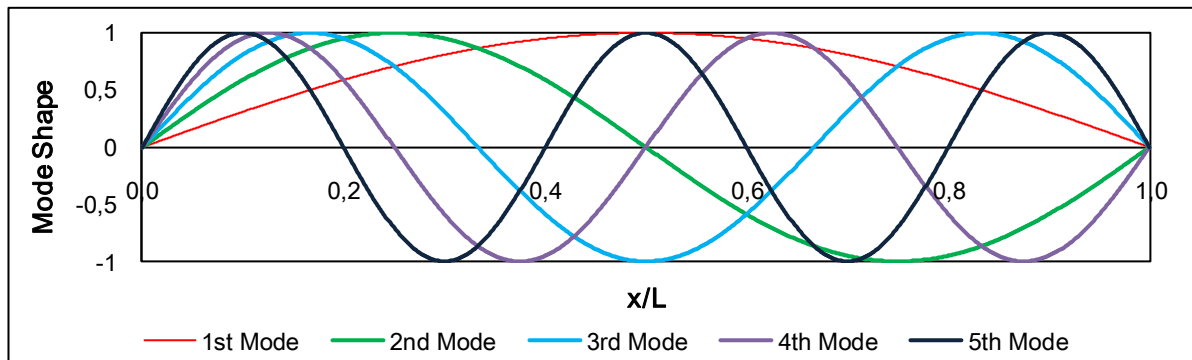


Fig. 1. First five mode shape for both ends are simply supported microbeam.

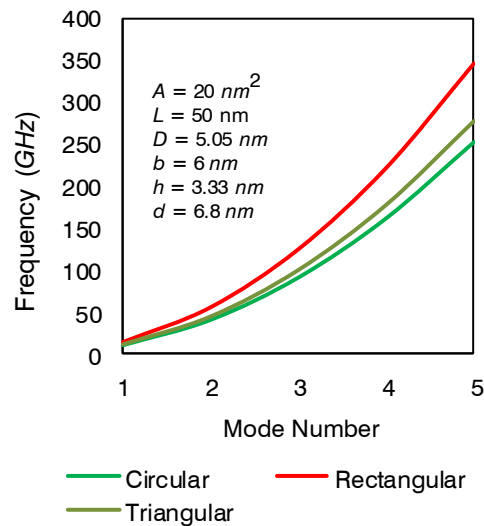


Fig. 2. Natural frequency values for different cross-sections and first five mod numbers

5. Concluding remarks

Free vibration analysis of gold nanowire is presented. By using continuum beam theory, the governing equation is obtained for Au nanowire. Then frequency and mode shapes obtained for different parameters. Frequency values are increased with the increasing value of mode numbers. Rectangular cross-section has biggest frequency value for Au nanowires using same cross-section area. Also, circular nanowire has smaller frequency value than the rectangular and triangular.

Acknowledgements

The financial support of the Scientific Research Projects Unit of Akdeniz University is gratefully acknowledged.

References

- [1] Li, Y., Song, J., Fang, B., Zhang, J., Surface effects on the postbuckling of nanowires, *J Phys D: Appl Phys*, 44, 425304, 2011.
- [2] Wang, D., Zhao, J., Hu, S., Yin, X., Liang, S., Liu, Y., Deng, S., Where, and how, does a nanowire break?, *Nano Letter*, 7, 1208, 2007.
- [3] Wang, Z., Zu, X., Gao, F., Weber, W.J., Atomistic simulations of the mechanical properties of silicon carbide nanowires, *Phys Rev B*, 77, 224113, 2008.
- [4] Miller, R.E., Shenoy, V.B., Size-dependent elastic properties of nanosized structural elements, *Nanotechnol*, 11, 139, 2000.
- [5] Kutucu, B., Nanoteknoloji ve Çift Duvarlı Karbon Nanotüplerin İncelenmesi, Yüksek Lisans Tezi, İstanbul Teknik Üniversitesi, Fen Bilimleri Enstitüsü, 2010.
- [6] Uzun, B., Karbon Nanotüplerin Kiriş Modeli ve Titreşim Hesabı, Lisans Tezi, Akdeniz Üniversitesi, 2016.
- [7] Yetim, A., Karbon Nanotüpler, Yüksek Lisans Tezi, Çukurova Üniversitesi, 2011.
- [8] Wei, G.W., Discrete singular convolution for the solution of the Fokker-Planck equations. *J Chem Phys*, 110, 8930-8942, 1999.
- [9] Wei, G.W., Solving quantum eigenvalue problems by discrete singular convolution, *J Phys B: At Mol Opt Phys*, 33, 343-352, 2000.
- [10] Wei, G.W., Discrete singular convolution for the Sine-Gordon equation, *Physica D*, 137, 247-259, 2000.
- [11] Wei, G.W., A unified approach for the solution of the Fokker-Planck equation, *J Phys A:Math Gen*, 33, 4935-4953, 2000.
- [12] Wei, G.W., Wavelets generated by using discrete singular convolution kernels, *J Phys A:Math Gen.*, 33, 8577-8596, 2000.
- [13] Wei, G.W., Zhang, D.S., Althorpe, S.C., Kouri, D.J., Hoffman, D.K., Wavelet-distributed approximating functional method for solving the Navier-Stokes equation, *Comp Physics Commun*, 115, 18-24, 1998.
- [14] Wei, G.W., Kouri, D.J., Hoffman, D.K., Wavelets and distributed approximating functionals, *Comp Physics Commun*, 112, 1-6, 1998.
- [15] Zhao, S., Wei, G.W., Xiang, Y., DSC analysis of free-edged beams by an iteratively matched boundary method, *J Sound Vibr*, 284, 487-493, 2005.
- [16] Hou, Z.J., Wei, G.W., A new approach to edge detection, *Pattern Recognit*, 35, 1559-1570, 2002.

- [17] Lim, C.W., Li, Z.R., Xiang, Y., Wei, G.W., Wang, C.M., On the missing modes when using the exact frequency relationship between Kirchhoff and Mindlin plates, *Adv Vib Eng*, 4, 221-248, 2005.
- [18] Lim, C.W., Li, Z.R., Wei, G.W., DSC-Ritz method for high-mode frequency analysis of thick shallow shells, *Int J Num Methods Eng*, 62, 205-232, 2005.
- [19] Civalek, Ö., An efficient method for free vibration analysis of rotating truncated conical shells, *Int J Press Vessels Pip*, 83, 1-12, 2006.
- [20] Civalek, Ö., Three-dimensional vibration, buckling and bending analyses of thick rectangular plates based on discrete singular convolution method, *Int J Mech Sci*, 49, 752-765, 2007.
- [21] Civalek, Ö., Nonlinear analysis of thin rectangular plates on Winkler-Pasternak elastic foundations by DSC-HDQ methods, *Appl Math Model*, 31, 606-624, 2007.
- [22] Civalek, Ö., Free vibration analysis of composite conical shells using the discrete singular convolution algorithm, *Steel Compos Struct*, 6(4), 353-366, 2006.
- [23] Civalek, Ö., Numerical analysis of free vibrations of laminated composite conical and cylindrical shells: discrete singular convolution (DSC) approach, *J Comp Appl Math*, 205, 251– 271, 2007.
- [24] Civalek, Ö., Korkmaz, A., Ç Demir, Ç., Discrete singular convolution approach for buckling analysis of rectangular Kirchhoff plates subjected to compressive loads on two-opposite edges *Adv Eng Softw*, 41, 557-560, 2010.
- [25] Gürses, M., Akgöz, B., Civalek, Ö., Mathematical modeling of vibration problem of nano-sized annular sector plates using the nonlocal continuum theory via eight-node discrete singular convolution transformation, *Appl Math Comput*, 219, 3226-3240, 2012.
- [26] Gürses, M., Civalek, Ö., Korkmaz, A.K., Ersoy, H., Free vibration analysis of symmetric laminated skew plates by discrete singular convolution technique based on first-order shear deformation theory. *Int J Numer Method Eng*, 79, 290-313, 2009.
- [27] Civalek, Ö., Nonlinear dynamic response of laminated plates resting on nonlinear elastic foundations by the discrete singular convolution-differential quadrature coupled approaches, *Compos Part B: Eng*, 50, 171-179, 2013.
- [28] Civalek, Ö., Diferansiyel Quadrature Metodu ile Elastik Çubukların Statik, Dinamik Ve Burkulma Analizi, XVI Mühendislik Teknik Kongresi, Kasım, ODTÜ, Ankara, 2001.
- [29] Civalek, Ö., Ülker, M., HDQ-FD integrated methodology for nonlinear static and dynamic response of doubly curved shallow shells, *Struct Eng Mech*, 19(5), 535-550, 2005.
- [30] Civalek, Ö., Nöro-Fuzzy Tekniği ile Dikdörtgen Plakların Analizi, III. Ulusal Hesaplamalı Mekanik Konferansı, 1998.

- [31]Mercan, K., Civalek, Ö., Buckling Analysis of Silicon Carbide Nanotubes (SiCNTs), *Int J Eng Appl Sci*, 8 (2), 101-108, 2016.
- [32]Demir, Ç., Civalek, Ö., Nonlocal Finite Element Formulation for Vibration, *Int J Eng Appl Sci*, 8(2), 109-117, 2016.
- [33]Demir, Ç., Civalek, Ö., Nonlocal deflection of microtubules under point load, *Int J Eng Appl Sci*, 7(3), 33-39, 2015.
- [34]Akgöz, B., Civalek, Ö., Analysis of microtubules based on strain gradient elasticity and modified couple stress theories, *Adv Vib Eng*, 11(4), 385-400, 2012.
- [35] Rao S.S., *Vibration of Continuous Systems*, John Wiley & Sons, 2007.